

Cold nuclear fusion theories

Exploration of exotic hydrogen states

Joel Simion Armelius



A thesis submitted in partial fulfilment of the
requirements for the degree of Master of Science in
the subject of Energy Technology

Geophysical Institute
University of Bergen
Bergen, Norway
April 10, 2018

Foreword

As far back as 2007, I was an eager high-school student pondering and reading about different breakthrough clean energy technologies I found all around the internet. After reading wide and far, I stumbled upon cold fusion. I was at the time convinced that this energy source would very soon put an end to both war and global warming although the sea of underlying physical mechanisms proposed always gave me a headache as they never seemed to agree. When telling my friends about what I thought was an imminent energy revolution they were seemingly impressed, but as they thought we could not make a difference they didn't pay much attention, and nothing was really done beyond that. I realised that I would need an alternative approach and in 2010 it dawned on me that others would probably use a sharper ear and be more intrigued if I had studied the subject. I was aware that studying cold fusion at a university was probably not possible based on its turbulent and stigmatized history. Of course the headaches I had previously incurred neither served as further motivation to study the disputed sea of suggested theories. I therefore concluded that I would by-pass the actual physics and instead focus on technology application, relying on physicists to develop a theory when the unexplained energy source was powering their lives. I started studying energy technology engineering at the Bergen University College, where I thrived learning about how our world machinery actually works. I wanted to write my bachelor thesis on cold fusion, but was quickly reminded that "if it sounds too good to be true, then it probably is" by the head of department. I accepted this for the time being and finished my bachelor degree, writing a thesis about thermodynamics, confident that my words would still carry slightly more depth now than before. During the three bachelor years, reports seemingly further stating the viability of cold fusion had become available, which motivated continued studies of energy technology. Healthily though, I had developed respect to theory as an essential part of technology development and application. This was a major factor to why I commenced on the masters program in energy technology at the University of Bergen. Here I thrived during the first year with great classmates and subjects, though when time to choose dissertation approached I encountered a profound challenge. My purpose for studying energy technology had been to add weight to my words on cold fusion, so ideally I would also write my thesis about the subject. During the past years however I had established a local "green shift" network, in which I was lucky enough to be granted a career relevant topic on hydrogen safety. To put a story short, subtle factors made me eventually decide to write about cold fusion in favor of the sensible and career strengthening alternative, though the hurdle of choice set me back a semester. At the university, I had been fishing for conversations about a newly discovered approach to cold fusion that I had come across, hoping to find someone who could further motivate and help me formulate an issue on the topic. I realised that it was a long shot considering the previous response I got while searching for a bachelor thesis on the subject, but for some reason, my words now apparently carried more depth as my supervisor Bjørn Johan Arntzen actually listened to me. By sheer luck, the first professor he introduced me to, Ladislav Kocbach, had through his curiosity already peripherally heard about the same approach as I had. Sadly for my headaches though, he was a professor in atomic physics, quantum mechanics and numerical tools among other physics heavy subjects. His sober response to my proposal of world peace and abundant energy was that, even though those were impeccable ideals, a masters dissertation is a rather small piece of concrete research. Some conversations later however, he had actually formulated a potentially relevant research topic. To him it was a conundrum that no one had already conducted this research as it was so "simple" in his mind. That was where my physics journey started. I knew next to

nothing with my engineering background, and was frightened by almost every word he said. I soon realised that I would be needing some insight in quantum mechanics and learn to use computers to simulate physical systems. I started studying quantum and classical mechanics through textbooks and MIT open courseware among a multitude of other online resources and gradually realised that it was not as bad as my headaches had predicted. I knew my time was limited and I could only hope that I would be able to attain enough knowledge to carry out this analysis. Thankfully Kocbach guided me through the jungle and pointed me in the right direction, which was critically needed as I far too often found myself completely surrounded by algebra and complicated expressions. I could not have attempted even part of this work without the guidance he has provided. I humbly thank you for your extreme patience with me and your firm belief that I could actually understand the subject and carry out this work. I never thought I would accomplish what I have during this year, and I am truly grateful for the opportunity and the new knowledge I have been given. This is more than a dissertation to me, as it is a part of a personal journey on a topic which I for a long time have been eager to explore.

Contents

| | | |
|----------|--|-----------|
| 1 | Introduction | 1 |
| 2 | Nuclear and atomic physics | 5 |
| 2.1 | Nuclear fusion as energy resource | 5 |
| 2.2 | Governing mechanisms for nuclear fusion | 5 |
| 2.2.1 | The electric force | 5 |
| 2.2.2 | The nuclear force | 6 |
| 2.2.3 | The Coulomb barrier | 7 |
| 2.2.4 | Potential barrier penetration | 7 |
| 2.2.5 | Reaction cross section | 8 |
| 2.3 | Nuclear fusion fuel impact | 9 |
| 2.3.1 | Nuclear binding energy | 9 |
| 2.3.2 | Fuels and reaction probability | 10 |
| 2.3.3 | Nuclear waste | 11 |
| 2.4 | High temperature nuclear fusion technologies | 11 |
| 2.4.1 | Magnetic confinement fusion | 11 |
| 2.4.2 | Inertial confinement fusion | 13 |
| 2.4.3 | Z-pinch | 14 |
| 2.5 | Low temperature nuclear fusion processes | 14 |
| 2.5.1 | Spontaneous fusion | 14 |
| 2.5.2 | Spontaneous muon catalysed fusion | 15 |
| 2.6 | So called ultra-dense deuterium | 15 |
| 2.7 | Relative distances | 16 |
| 3 | Quantum physics | 17 |
| 3.1 | Quantum Chemistry | 17 |
| 3.2 | The Schrödinger equation | 17 |
| 3.3 | The wavefunction | 19 |
| 4 | Method for determining bound states | 23 |
| 4.1 | Solving the Schrödinger equation | 23 |
| 4.2 | Nuclei arrangement and repulsion | 25 |
| 4.3 | Potential energy felt by electrons | 26 |
| 4.3.1 | Potential terminology | 27 |
| 4.3.2 | Soft Coulomb potential | 28 |
| 4.3.3 | Truncated Coulomb potential | 29 |
| 4.4 | Numerical tools | 30 |
| 5 | Results | 33 |
| 6 | Discussion | 35 |
| 7 | Conclusion and future perspectives | 39 |
| | Appendices | 43 |

| | | |
|----------|--|-----------|
| A | Repulsion in a string | 43 |
| B | Matlab code | 44 |
| B.1 | Numerical Schrödinger equation | 44 |
| B.2 | Truncation value optimization | 45 |
| B.3 | Potential | 46 |
| B.4 | Repulsion | 47 |
| B.5 | Main analysis program | 47 |

Nomenclature

Latin symbols

| | |
|-------|---|
| E | Energy |
| F_e | Electric force |
| H | Hamiltonian operator in quantum mechanics |
| k_e | Coulomb constant |
| V | Eigenvectors |

Greek symbols

| | |
|------------|-------------------------------------|
| Δ | Change between two states |
| Λ | Eigenvalue matrix |
| ∇ | Gradient operator |
| ∂ | Partial derivative |
| Ψ | State function in quantum mechanics |
| σ | Reaction cross section |

Acronyms

| | |
|------|----------------------------------|
| CMNS | Condensed Matter Nuclear Science |
| IEA | International Energy Agency |
| LENR | Low-Energy Nuclear Reactions |
| PES | Potential Energy Surface |
| UFL | Upper Fusion Limit |
| WEO | World Energy Outlook |

Abstract

Nuclear fusion technologies hold the potential to revolutionize the way we produce energy on earth. It is an opportunity to lift our current dependency on external factors such as weather and fossil reserves while producing vast amounts of emission free energy. For more than two generations, several novel ways to extract fusion energy have been proposed and attempted.

One recently suggested approach is based on an assumed aggregate of deuterium named ultra-dense deuterium. The existence of this aggregate seems to follow from experimental observation of ejected fragments with relatively high kinetic energy. Uncertainties connected with the nature of the yet hypothetical ultra-dense state, call for further investigations as the present explanations are vague and third party verifications have so far not been completely independent.

The focus of this study has been to investigate a possible aggregate of hydrogen which could lead to the reported ejected particle energies. The present results provide an independent model analysis based on well known physics and aims to further enlighten the subject and eventually encourage continued studies. The nuclei are said to be metastable at a very small distance compared to a regular molecule, much like the exotic muonic molecule which is well known to catalyze fusion due to the small distance between the nuclei. In this thesis a one-dimensional numerical model has been created based on quantum chemistry to analyze the energetic stability of a proposed hydrogen aggregate.

The results show that there may indeed exist a quasimolecular system where nuclei are stable at around $1/24$ the distance of a regular hydrogen molecule. The nuclei must be axially aligned and of single charge to minimize repulsion, and also a certain minimum number of nuclei is required, found to be 17 in the model.

The distance between the nuclei is an order of magnitude larger than observed in the muonic molecule, limiting though not removing the probability of fusion which decreases exponentially with increasing distance. The results point toward a need of further investigation through a three-dimensional model of the state which would eliminate much of the uncertainty inherent in the current model.

1 Introduction

The world today is heavily and increasingly dependent on the continuous supply of energy. Humans are on their own rather puny creatures with limited powers, however our intellectual capacity has allowed us to manipulate the world around us to a degree where one human can output an extraordinary amount of work through the use of technology. Machines require input of external energy to function, energy which we have become masters of transforming from raw materials and natural processes into mechanical or electrical energy. As more of the human population acquire the means for exploiting machines to do work, the energy requirement continues to increase. Currently the world's energy demands are met by the exploitation of a variety of sources, though the bulk energy comes from depletable fossil reserves. British Petroleum annually produce a review [1] on the world energy status where they present global primary energy consumption of commercially traded fuel types, see Fig. 1. Primary energy represents the energy of a source before it has been refined in any way, such as raw oil, wind, elevated water etc. The review shows that the bulk harvested energy in 2016 was based on fossil fuels (85.5% excluding nuclear), dominated by oil, coal and natural gas. The renewable sources hydro, wind, solar and geothermal accounted for 10.0% whereas nuclear power, currently produced in fission reactors classified as a fossil fuel, represent 4.5% of the primary energy consumption.

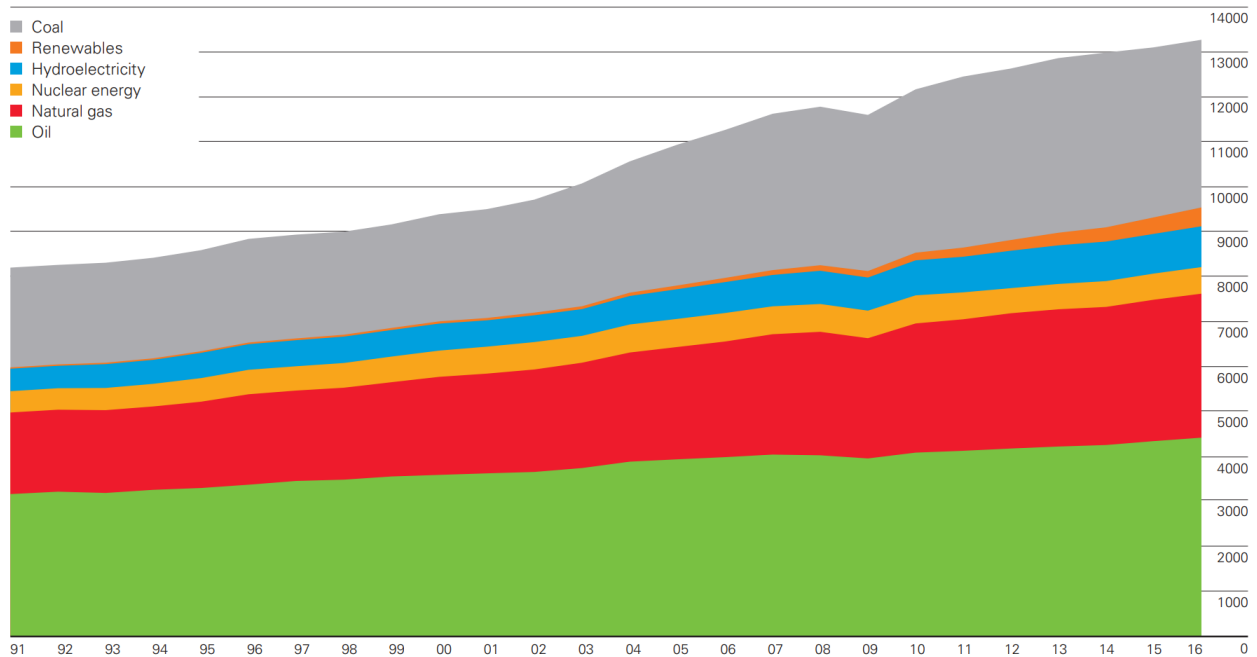


Fig. 1: BP Statistical Review of World Energy, World primary energy consumption [1]. Horizontal axis shows years and vertical axis shows energy measured in Mtoe, Million Tonnes of Oil Equivalent.

These figures illustrate that the world today is heavily dependent on fossil fuels to meet energy demands. They may also serve to realise the scope of the challenge ahead as fossil reserves on earth inevitably will deplete. In recognition of fossil fuel depletion and the environmental impact of carbon emissions, focus is seen shifting to the development and deployment of renewable energy technology.

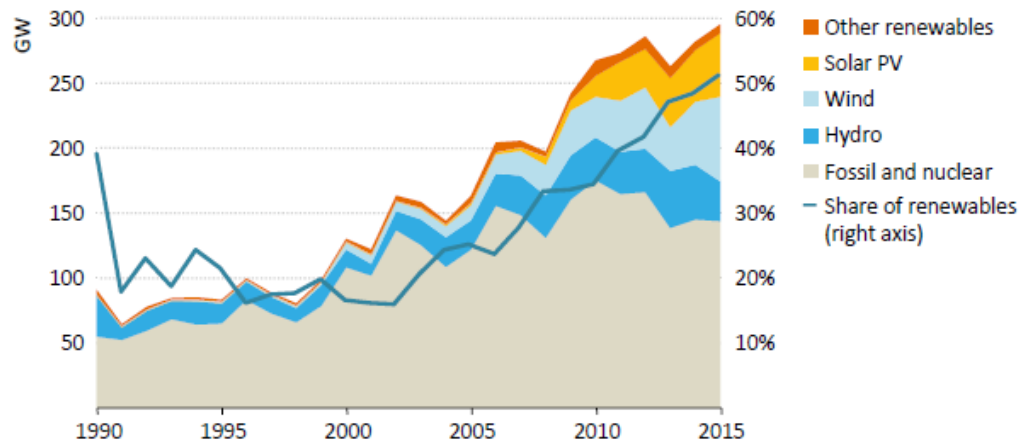


Fig. 2: World Energy Outlook 2016, installed capacity of different energy sources [2].

The International Energy Agency (IEA) World Energy Outlook (WEO) presentation of annual global power deployment depicts technology shares of installed capacity in Fig. 2 from 1990 to 2015. The year 2015 was pivotal as the first time in history when installed renewable capacity exceeded that of fossil power. This shows that there is already momentum in the deployment of renewable sources. The increasing share of renewable sources is influenced by both policies to reduce carbon emissions and by the rapid advances seen in renewable technology over the last decade. Through the work of the United Nations Framework Convention on Climate Change, the Kyoto protocol was the first major global agreement on carbon emissions reduction, with a top down approach setting binding emission reduction targets for all participating nations. In november 2016, the Paris Agreement was established and went into effect. This is the first properly comprehensive climate agreement counting only 25 pages, and with a "bottom up" structure, its emphasis is on consensus building, allowing the participating nations to set targets based on their specific situation and capacities. Thus it is more of an executive agreement fostering political encouragement to induce nation specific plans for change, rather than a treaty of regulations. The major aim of the agreement is to limit global temperature rise to "well below 2 °C above pre-industrial levels and pursuing efforts to limit the temperature increase to 1.5 °C" [3]. Article 10 of the agreement discuss technology development, and clarifies that "Parties, noting the importance of technology [...], shall strengthen cooperative action on technology development and transfer". Furthermore the article promotes the long term importance of accelerating, encouraging and enabling innovation, in particular for early stages of technology, as effective response to meet the challenges of climate change. This attitude is further encouraged by the IEA ministers, who state that "Our countries have a vital role in helping to develop new, breakthrough technologies and helping to enable emerging energy technologies to become technically and commercially viable" [4]. These agreements along with current increasing deployment of renewable energy are clear indications that there is global awareness and commitment to face the fundamental challenges of our time. However, as also pointed out in the IEA WEO, the challenges associated with the temperature goal of 1.5 °C are stark; even though the development of key technologies is seen already, the phase of deployment still lacks momentum and falls short of even the 2 °C goal [2]. As the average temperature in the first half of 2016 already was 1.3 °C above the average in 1880 [5], the aim of the Paris Agreement might seem ambitious or even unrealistic. To meet this goal, the IEA states that net-zero carbon emissions around 2040 will be required and

every known technological, behavioural and regulatory means to reduce or replace carbon emissions must immediately be deployed [2]. This leaves us in a situation where renewable energy, though mainly wind and solar power for the time being, indeed is in focus and fossil fuels are being phased out, though as we saw in Fig. 1, the fossil gap to be filled by emission free and safe energy technology is large.

It is then clear then that the severity of the challenge is recognised and that if measures to meet these are to be established, development of new energy technology is critical. Ideas must be nourished through recognition of environmental and energy security concerns. There have been many ideas on how to produce clean energy through the years, though few of them have been properly acted upon. One rather fundamental approach, suggested as far back as the 1950's, was to mimic the mechanism of the sun in producing fusion energy. Technologies utilizing fusion could produce millions of times more energy than fossil fuels. A reminder of the energy potential of nuclear reactions can be seen in existing fission reactors which undeniably produce vast amounts of energy, though unavoidable safety and environmental concerns regarding accidents and waste disposal limit their widespread use.

Scientists promoting nuclear fusion do so advertising the technology as safe, reliable and fuel abundant. There are about a hundred research facilities worldwide, with the most prominent currently being built in France [6]. There are currently two mainstream paths to achieve fusion, while in the past there were alternatives being investigated. The main two approaches being developed today both include very high temperatures, in the order of 100 000 000 °C. The past alternative paths included much lower temperatures and were commonly referred to as "cold fusion". Since 1989 cold fusion has been disregarded by the majority of scientists as "pathological science". Cold fusion is by many still viewed as an infection of the mind, comparable to the alchemists search of the philosophers stone during the Medieval Age. Scientists who in the past openly pursued cold fusion had their careers more or less ruined, leading to very limited research in the field.

To understand why cold fusion has been such a sore scientific subject, to the extent where mentioning the words could make fellow physicists laugh, instantly disregard ones credentials or advice to avoid research for the sake of ones career (as happened to me), a brief presentation of the events in 1989 is needed. I will not attempt to find credible sources, as this would be a waste of time as historically any source seems to be subject to skepticism regardless of author. Following in this paragraph is a short presentation of what can be found in a wikipedia article on cold fusion: Martin Fleischmann was at the time a revered world leading electro chemists. He and Stanley Pons, then chairman of the chemistry department at the University of Utah, were investigating the idea that fusion of deuterium loaded on a palladium surface at low temperature could be possible due to extreme pressures known to be present in such loaded surfaces. Their experiments showed that a test glass containing a palladium electrode exposed to a voltage in a deuterium bath could suddenly increase liquid temperature by some tens of degrees. This was very exciting, but their physical explanation was not clear beyond that the reaction could not be of purely chemical nature due to the high energy released. This led them to question whether nuclear reactions could be present. They were planning to release a research article when the University of Utah in March 1989 prematurely released their papers and held a press conference announcing the discovery of this groundbreaking research, apparently against an agreement with the two chemists. The two were aware that this technology could be a disruptive "game changer", and originally wanted to carefully open the door to the research area as it was not yet understood. The response to the press conference was a massive global media outburst proclaiming cold fusion as discovered and available.

Immediately attempts to replicate the effect commenced at chemistry labs across the world. The experimental protocol was not yet published, and the physics explaining the phenomenon was not clear. Of course replications were predetermined to fail due to this lack of setup and understanding. That is exactly what happened as consistency in the results of replicators was largely absent. Turmoil developed during the spring of 1989 as some groups replicated the effect, while others got nothing or a slight effect sometimes. In short, the lack of consistent reproducibility and vague explanations shifted the media to refer to the phenomenon as "cold confusion" rather than cold fusion as scientific debate flared, moving the focus from continued research over to debating the viability of each others measurements and theories. Eventually the field gained the reputation of being "pathological science". Scientific articles started to be rejected without consideration and soon main stream scientific research came to a halt as it could be a devastating endeavour to a scientific career.

Since 1989 cold fusion research has been mostly absent in accredited journals, even though research in the field has far from seized to proceed. As mainstream research in the field was avoided, researchers still devoted were isolated and often dubbed "believers" of the field, which generally does not resonate well when conducting scientific research. Those who continued research came in contact and in 2004 eventually formed an international society where they could freely exchange ideas and development. The field has been re-branded and is now referred to primarily as one of the two definitions Low-Energy Nuclear Reactions (LENR) or Condensed Matter Nuclear Science (CMNS).

A possible reason why research in cold fusion is disregarded is that the community is under pressure due to a history of outer skepticism and disbelief, thus normal procedures of scientific work are not followed. The inner criticism is suppressed by the overwhelming outer pressure and even the peer-review process - when active - is weakened by this. Thus the standards and reliability of the published research as a whole are rather low. It is tolerated to publish texts on subjects under dispute, however often in earlier papers on cold fusion, requirements of reproducibility, quality of theoretical models and their detailed assumptions can often be criticized and all this makes it difficult for a scientist outside of this community to identify really valid results. The recurring factor is that the lack of an acceptable theoretical explanation has limited the communication between those who pursue the subject and those who need persuading.

In more recent history, there has been research conducted in Sweden on so called ultra-dense deuterium. The researchers try to avoid being associated with cold fusion or LENR, though considering the implications of their research it is arguably the most promising approach to understand the phenomenon, should it be real. Theoretical analysis of a possibly ultra-compressed hydrogen aggregate is the issue addressed in this thesis, as such an analysis has not yet been made. Further details on ultra-dense deuterium research and the current issue is presented later in this thesis.

This thesis is structured to present aspects of atomic physics relevant to nuclear fusion in section 2, where selected approaches to achieve fusion are also covered. Finally section 2 presents previous work on ultra-dense deuterium and the issue of this thesis, which is the focus of the following sections; Section 3 provides necessary quantum chemistry theory, where the focus is on molecular stability through use of the Schrödinger equation. Section 4 presents a method of using previous theories to develop a numerical model for the analysis. In section 5 the results are presented, which are discussed in section 6 in connection with previous work and inherent limitations of the current model. The conclusion sums up the results and suggests future work.

2 Nuclear and atomic physics

This section presents nuclear fusion as a potential source of energy. The physical mechanisms governing nuclear fusion are presented and some technical approaches are presented briefly before concluding with a review on previous relevant work in the field of dense aggregates of deuterium.

2.1 Nuclear fusion as energy resource

Nuclear fusion is the process in which two nuclei join together to form one larger nucleus and usually some fragments. The primary reasons why fusion energy is a compelling source of energy are the following: First, the process releases large amounts of energy. Second, the fuel is cheap, abundant and available anywhere on earth. Third, the process produces no long-lived radioactive waste. Fourth, the reactors are inherently safe as uncontrollable chain reactions are impossible [7], rendering proliferation impossible. With that said, the major challenge of today is developing appropriate technologies to facilitate the process.

Fusion reactions release nuclear binding energy as heat according to Einsteins equation $E = mc^2$ which states that any change in mass m corresponds to a change in energy E , with proportionality constant c being the speed of light. When fusing light nuclei together, the products will have a lower mass than the sum of their former constituents, thus a change in energy must also occur. To illustrate this energy potential, a common fusion reaction of two deuterium nuclei ${}^2_1\text{H}$ is presented, with the resulting products for this example being a tritium nucleus ${}^3_1\text{H}$, a protium nucleus (proton) ${}^1_1\text{H}$ and excess energy. Normally the reaction has two outcomes of equal probability though only one is shown here for simplicity:



The mass difference of the reactants and products indicate the binding energy released per fusion reaction which can be evaluated using $E = mc^2$. The energy release per kilo deuterium fuel when considering the real reaction with two outcomes, is about 55 GWh/kg of heat, which is more than twice the energy released during fission of one kilo uranium [8]. Compared to a kilo of gasoline, which upon combustion releases about 13 kWh/kg, the nuclear fusion of deuterium produces 4.2 million times more energy.

Fusion may occur if two nuclei are brought very close, to a length scale corresponding to near nucleus dimensions although at the length scale in question, effects of quantum mechanics cannot be neglected. When adding the possibility for quantum tunneling, the high energy required through classical calculations overshoot the real world requirements.

2.2 Governing mechanisms for nuclear fusion

To understand what a technology must achieve when aiming to produce excess energy through nuclear fusion, the governing mechanisms enabling nuclear fusion are presented.

2.2.1 The electric force

The electric force, also called the Coulomb force, acts between charged bodies. Charles Augustin Coulomb (1736-1806) established the physical relation in 1784 that predicted this force, which was

named Coulomb's law in recognition of his work:

$$F_e = k_e \frac{|q_1||q_2|}{r^2} \quad (2.2)$$

If the coulomb constant k_e is $8.9876 \times 10^9 \text{ Nm}^2/\text{C}^2$, q_1 and q_2 being the respective charges of the interacting bodies in units of coulombs and r set as distance between the charges in meters, then F_e is the scalar magnitude of the electric force measured in newtons. A directional unit vector from one charge to the other may also be included, convenient if the net contribution of multiple charges at different locations are to be evaluated. This vector will either point inward (from one charge toward the other) or outward depending on the signs of the charges. For two particles with charge of the same sign, the electrostatic force is repulsive, thus the force vector points from one charge away from the other. Similarly for charges of opposite sign, the force vector becomes negative which brings the particles together. The closer the bodies, the stronger the force. Though quickly decreasing with distance, the force is long reaching and acts accumulative, meaning that one proton approaching a nucleus experiences an accumulated electric repulsion from all other protons in the nucleus, which also repel each other. For this reason, fusion conditions are hard to achieve between large nuclei due to the accumulated electric repulsion resulting from multiple protons. On this basis the most promising nuclei for fusion are the smallest ones such as hydrogen and its isotopes deuterium and tritium, each holding only a single charge, minimizing repulsion.

2.2.2 The nuclear force

The nuclear force, also called the strong force is the force which pulls the nucleons together within the atomic nucleus. It is generally much stronger than the electric force, which is apparent since multiple protons can be confined in a stable manner within the nucleus without exploding due to the immense electric force between them. The force cannot be described by classical mechanics in a similar way as the electric force. Current understanding of the strong force is based on Quantum Chromodynamics, where quark interactions are fundamental to the approach. Historically most descriptions of the strong force have been approximations. One approximation, known as the Woods-Saxon potential, describes a mean field potential for the nucleons in the atomic nucleus. Another called the Yukawa potential, rely on particles masses to determine the reach of the force. The Yukawa potential can also be used to describe the Coulomb potential.

By qualitative description, the strong force is very short ranged and it does not accumulate in the presence of multiple nucleons. That means that each nucleon within the nucleus interacts only with its nearest neighbour, which corresponds to the force reaching about 1 fm (10^{-15}m) or less [8]. In elements where there are many protons, the repulsive long reaching electric force accumulates while the nuclear force does not. By having very many protons, the nucleus can become unstable and eventually the electric repulsion may overcome the nuclear force and cause the nucleus to break up through nuclear fission into smaller, more stable elements. In nature, this is accounted for by adding more neutrons, which increases the distance between the protons which reduces the repulsive force between them. This is the reason why there are more neutrons than protons in elements heavier than iron [9]. A curious note on the nuclear force as outlined in [10] is that the nuclei should collapse if the force was only attractive. As this is obviously not the case, another property of the force must exist; the nuclear force is *repulsive* at very short distances, which helps explain why the volume of the nucleus is proportional to the number of nucleons inside it. Based

on this, the force can be visualized as a glue between solid particles. For fusion reactions, this is an important notice as it helps to understand the distance required to achieve fusion. The fusing particles must essentially come in contact with each other before they feel the strong force.

2.2.3 The Coulomb barrier

The Coulomb barrier represents the interplay of the two forces mentioned above and is a convenient way to visualize initial requirements for fusion. The electric potential energy increases inversely with distance as e.g. a proton approaches the nucleus, and the nuclear force comes into play and dominates only when the proton comes really close to the nucleus. Fig. 3 shows a sketch to visualize the barrier, though the energies in the illustration are not in proportion. For an incoming proton from the right, it loses velocity as it "climbs" the repulsive barrier, before it gets accelerated into the nucleus if it goes over the top. This can be visualized as a ball rolling over a hill, slowing down on the way up and then accelerating again once over the top. This "electromagnetic hill" is often referred to as the Coulomb barrier. The barrier represents the energy classically required to obtain fusion, and must be dealt with in an appropriate manner in any fusion technology.

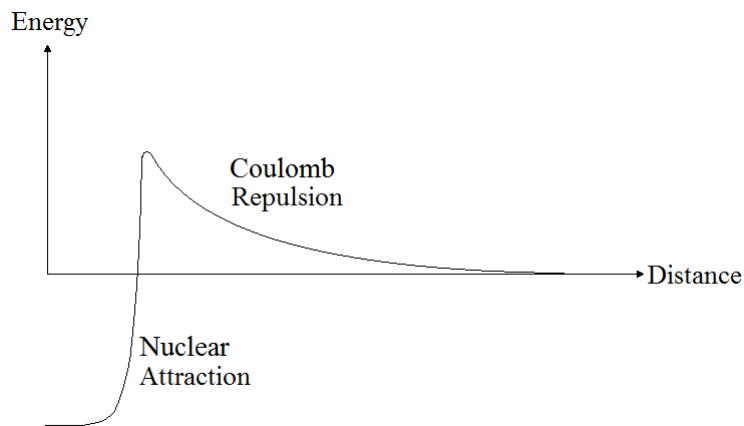


Fig. 3: Sketch of the Coulomb barrier as a combination of electric repulsion and nuclear attraction.

2.2.4 Potential barrier penetration

Potential barrier penetration, also called quantum "tunneling", is a phenomenon that arises in the domain of quantum mechanics. It is commonly known as the ability to overcome a barrier by tunneling through it rather than overcoming it, see Fig. 4. The effect of quantum tunneling is only present in very small scale, as its probability decreases exponentially with tunneling distance. The mechanism is a property of the quantum wave function and has a varying reach, typically below 100 pm (picometers) for the electron [9] and much smaller for nucleons. In classical mechanics, a ball going over a hill must have sufficient energy to reach the top. If however, the ball and hill were small enough, the ball could alternatively tunnel through to the other side. In the sun, tunneling is believed to be essential as the temperature and pressure alone is not enough to overcome the coulomb barrier. For fusion reactions on earth, the effect may enable fusion at energies below those calculated using classical mechanics where tunneling is not allowed.

Barrier penetration has several simplified representations, however the basic concept is that one treats a particle as a quantum mechanical wave, and analyses the given situation by solving

the Schrödinger equation for the region with the appropriate boundary conditions. The wave representation has a spatial dimension and must be continuous. If a particle i.e. the wave is approaching a potential barrier (visualize a wall), it may bounce off and be reflected. However, when the Schrödinger equation is solved for the case, the wave exists within the barrier though decays exponentially with distance inside it, and if the wall is thin enough, the wave also exists on the other side. The wave function actually represents possible locations where the particle may reside, which means that if the wave exists on the other side of a barrier, the particle can be present there. In thermonuclear fusion, one aims to increase temperature and thus the velocity, or kinetic

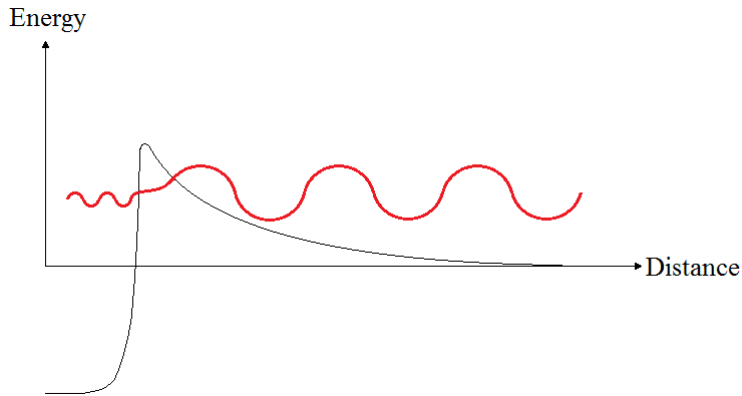


Fig. 4: Sketch to illustrate potential barrier penetration, or «tunneling» phenomenon.

energy, of the particles so that the collision energy is sufficient to overcome the the Coulomb barrier by tunneling. The time available for a particle to tunnel will largely affect the probability of the phenomenon to occur, where in thermonuclear reactors the particles are accelerated toward and bounce off each other if tunneling does not occur. This leaves a very limited time frame with only one approach providing the opportunity to tunnel. Another approach is to reduce the size of the atom or molecule so that the nuclei come close. This is the approach used in muon-catalyzed fusion, where high molecular density means the the nuclei have already climbed the Coulomb barrier by a substantial amount. The common denominator for all approaches is that they all aim to bring the nuclei close in order to increase the probability of fusion by quantum tunneling.

2.2.5 Reaction cross section

Reaction cross section is a general measure of reaction effectiveness, and not a mechanism in itself. It defines the ratio of one type of produced reaction product per time to the incoming particles with their associated velocity and the total number of nuclei available to react in the target volume:

$$\sigma(a, b) = \frac{N_b}{(n_a v)(n_t A \Delta x)} \quad (2.3)$$

N_b is the number of outgoing particles of type b in units s^{-1} , $n_a v$ is the number of incoming particles per unit volume with their associated velocity in units $m^{-3}ms^{-1}$ and finally $n_t A \Delta x$, the number of particles available to react per unit volume n_t times the volume available $A \Delta x$, is unit-less ($m^{-3}m^3$). This gives th reaction cross section units of m^{-2} . The cross section is usually presented as *barns*, where one barn is in the order of the nuclear radius R squared, $R^2 \sim 10^{-28} m^{-2}$. For each reaction, the cross section will be a function of the energy of the incoming particles [8]. The

reaction cross section is a valuable tool when considering different experimental setups as it is a convenient measure of desired output to required input, however it is not used any further in this project.

2.3 Nuclear fusion fuel impact

The governing mechanisms presented in previous section indicated that light nuclei are the primary candidates for nuclear fusion reactions. Other fuel dependent factors, such as binding energy release, probability of fusion and reaction products will also dictate reaction efficiency and choice of fuel. These factors are presented in this section.

2.3.1 Nuclear binding energy

Inside the nucleus, there are a number of nucleons in the form of neutrons or protons which are held together by the strong nuclear force. In order to separate these nucleons, energy must be added. The amount of energy required to separate the nucleons is called the nuclear binding energy. By energy conservation, the equivalent separation energy is released upon joining of nucleons so that the bond and nucleus forms. The binding energy can also be viewed in terms of mass, as free nucleons weigh more than those bound in a nucleus. The mass difference corresponds to the binding energy through the relation $E = \Delta mc^2$. As noted in section 2.2, nuclei with few protons have the lowest potential barrier and are thus most practical in fusion reactions. This is also convenient as the nuclear binding energy varies most between the lightest elements. For a deuteron, which consists of a proton and a neutron, the binding energy is rather small (2.2 MeV) due to the two nucleons having only one contact point between them if visualized as spheres. For helium, which has four nucleons (two neutrons and two protons) the bond is much stronger (28.3 MeV). This is because each nucleon within the nucleus can be thought of as being in contact with three neighbors in a tetrahedral configuration, resulting in six bonds. Picturing nucleons as spheres is not a correct representation, but it helps understanding why and how the binding energy changes between elements. This spherical representation of nucleons was first proposed by Niels Bohr in 1936, who by using what he called the liquid-drop model, was able to explain some general features of the nucleus [11].

For elements of many nucleons, binding energy can be visualized by how many contact points there are if nucleons were spheres. If there are many nucleons, all spheres cannot be in contact at once, and a repeating pattern is introduced though no extra contact points for each nucleon is made, meaning binding energy increases rather slowly with the addition of nucleons. Nucleons in the form of protons repel each other quite significantly at the distances involved. With an increasing number of protons, repulsive force increases and can eventually overcome the strong force between nucleons as the Coulomb force is accumulative and has long reach. The nucleus surface area on which no bonds are formed also grows when adding nucleons, which contributes to weaken the overall binding energy.

When schematically representing average nuclear binding energy per nucleon, as in Fig. 5, the binding energy is highest for the iron nucleus which consists of 56 nucleons. Adding more nucleons than this only contributes to making the average binding weaker. This means that fusing two nuclei heavier than iron is an endothermic reaction, absorbing rather than releasing energy. On this end of the scale, breaking a nucleus apart is what yields energy, as seen in fission reactors using elements from the right end of the binding energy curve. The overall relation to determine nuclear binding

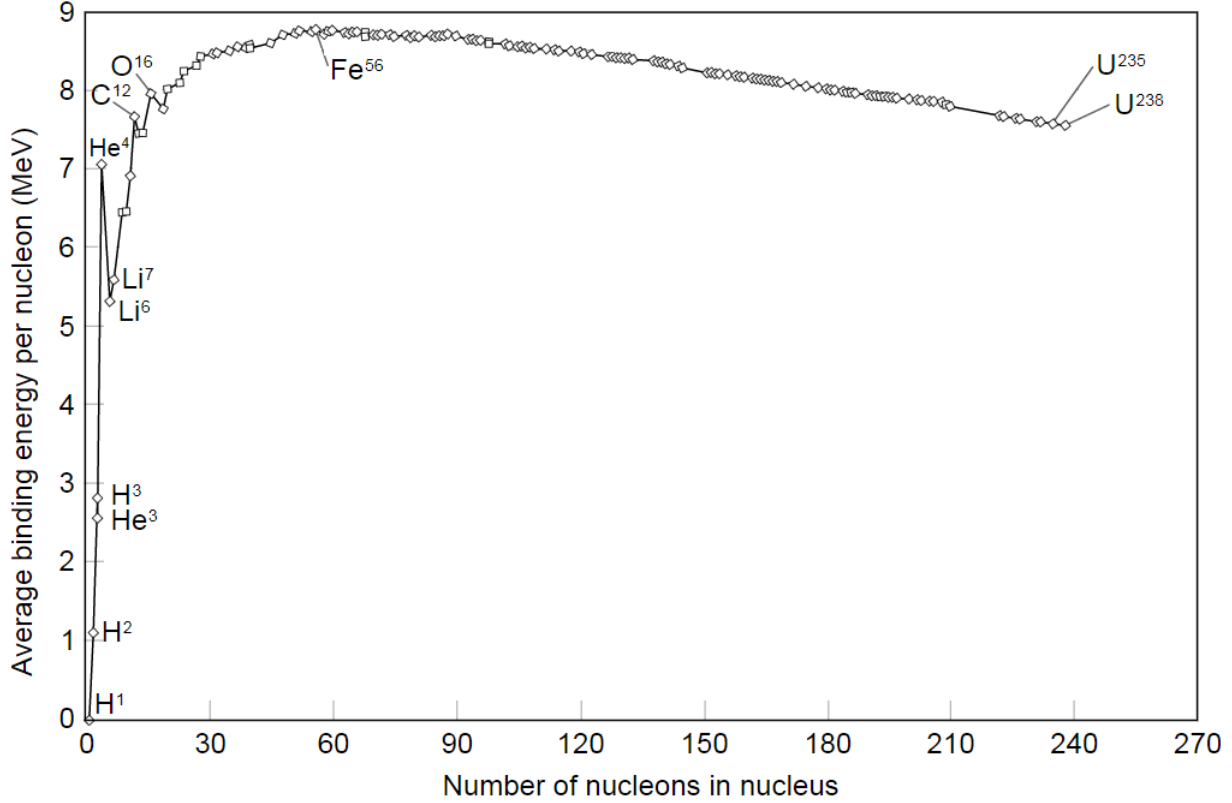


Fig. 5: Binding energy as function of number of nucleons. Image courtesy [12].

energy E_b is given by

$$E_b = [Zm_p + (A - Z)m_n - M]c^2 \quad (2.4)$$

Where Z is the proton count, A the nucleon count, m_p the proton rest mass, m_n the neutron rest mass, M the rest mass of the whole nucleus and c the speed of light. By using SI units, E_b results in units of Joules. The energy yield from fusion of two initially equal species is given by the change in binding energy $E_{b2} - 2E_{b1}$.

2.3.2 Fuels and reaction probability

There are multiple reactants available for fusion reactions, though deuterium is the current fuel of choice due to its natural abundance and low cost of preparing. Deuterium ${}^2_1\text{H}$ is the isotope of hydrogen which has one neutron in addition to the proton in its nucleus. For every 6700 hydrogen atoms in sea water, one has been replaced by a deuterium atom. This means that there is a lot of deuterium available in the oceans, providing a virtually inexhaustible fuel source. Also, the cost of extracting deuterium is minimal compared to the energy released by the fusion reaction [13]. The picture is more nuanced than this as there are several factors influencing the choice of fuel. The probability of fusion, or reaction cross section, varies with different reactants. Deuterium - Tritium fusion is the reaction with highest probability, thus making it the easiest to achieve. Tritium is the isotope of hydrogen with two neutrons instead of one as in deuterium. The products of D-T fusion however includes a fast neutron, which is an undesirable side effect as it radiates to the reactor chamber walls, degrading and making them radioactive for some time [6]. Tritium is not readily available as it is an unstable isotope, and if needed must be bred, usually from lithium. Lithium

is on the other hand widely available both in the earth crust and in the oceans [7]. Alternatives such as fusion of two hydrogen nuclei (protons) could be a simple and powerful process as it has the largest mass difference of any fusion reaction thus yielding the largest energy gain. This is the primary fusion reaction occurring in stars, but the probability of this reaction is extremely low as proton-proton fusion is dependent on weak interactions as one of the protons must transform into a neutron, which is a process of very low probability. This is good for us as it makes the sun burn slowly, though the low probability makes the approach unsuitable as a process for controlled fusion on earth. Alternatives such as a proton fusing with a neutron is a very simple reaction as the neutron carries no charge and has thus no potential barrier to overcome. This approach is however not suitable either, as free neutrons are rare and costly to produce [8].

2.3.3 Nuclear waste

One of the major differences of nuclear fusion, as opposed to fission where heavier elements are split up, is the absence of direct radioactive waste products. Still during the reactions, free neutrons may be produced and need to be shielded. This will influence the reactor walls which will be radioactive for some time and must be handled properly upon disposal. This material may have to be stored up to a century before recycling [6]. There is also a possibility for small tritium release to the atmosphere though this is considered a minor and placable hazard [14].

2.4 High temperature nuclear fusion technologies

Any fusion technology must deal with the governing mechanisms. Since 1950, development of controlled fusion technology has had two major approaches; magnetic confinement fusion and inertial confinement fusion. Both approaches have in common that they utilize high temperature or kinetic energy to achieve fusion. As high temperature fusion is not the focus in this thesis, this section covers mainly general concepts of more common high temperature technologies. Other approaches and variations do exist, though are not mentioned as they all rely on the same high temperatures.

2.4.1 Magnetic confinement fusion

Temperature of a gas can be described in terms of average particle kinetic energy by the relation $E_{ave} = \frac{3}{2}kT$ where $k = 1.3805 \times 10^{-23} \text{JK}^{-1}$ is the Boltzmann constant. In magnetic confinement fusion the goal is to maintain a plasma at a temperature required for fusion, in the order of 100,000,000 degrees Celsius. The required temperature can be found using the Coulomb force to evaluate potential energy at the distance required for fusion. By using the Boltzmann relation, the temperature corresponding to this energy can be calculated. Since no known material can withstand the required temperature, strong magnetic fields act as non-physical walls to hold the plasma in place. The main difficulty of this approach is that the plasma quickly tends to find a way to leak out of the confinement.

Maxwellian velocity distribution describes energy distribution of particles in a gas or a fluid, where some particles have greater energy than the average described by the Boltzmann relation. Even if the average temperature is too low for nuclear fusion, the upper tail of the velocity distribution curve represents a fraction of particles which may have high enough energy to overcome the barrier, even though the majority does not. This property is heavily relied upon in magnetic confinement fusion.

The Tokamak

The Tokamak (**toroidalnaya kamera magnitnaya katushka**, meaning toroidal chamber magnetic coils) is a magnetic confinement fusion device originally developed in Russia and first presented at the 1958 Geneva Conference. At the conference the Tokamak was a blunt device in comparison to the alternative Stellarator presented by the British and Americans. Over time, all other nations working on magnetic confinement fusion technology have adopted the Tokamak.

The machine works by confining the plasma in a magnetic torus. The magnetic field is shaped as a helical twist that runs around the torus shape. The helical field is a resulting superposition of two primary fields. One field is running along the torus in circles, and the other transverse to this around the torus small diameter. Since magnetic field lines are always perpendicular to a current, the first one that runs along the torus large diameter, called the toroidal field, is produced by many similar coils spread around the torus, encapsulating it. The other field is the poloidal one, generated by currents induced in the plasma itself. This is where the russians outsmarted the British and Americans, as they recognized and exploited the conductivity of the plasma itself. By introducing a large coil along the center axis of the torus, they were able to induce a large current in the plasma which produced a magnetic field perpendicular to the torus. The poloidal and toroidal magnetic fields combine to superimpose a helical field. This type of magnetic field is needed to confine the plasma, as particles otherwise tend to drift out of the confinement. A constraint of the Tokamak is that it must run on AC since the plasma current is essentially a transformer. Household AC has a frequency of about 50Hz, while one pulse in a fusion device may be several minutes long. Even though the pulses are long, this limits the machine in achieving continuous operation [15]. There are multiple stages of heating the plasma. The first is by the current (several million amperes) itself which runs through the plasma, this is called ohmic heating, possible since the plasma has some finite ohmic resistance due to electrons colliding with other particles when they are accelerated. As the particle velocity increases, the resistance decreases. Ultimately the plasma behaves like a superconductor and no further temperature increase can be achieved by ohmic heating. In order to further increase the temperature, neutral particles (neutral in order to penetrate the magnetic confinement) are beamed into the plasma where they collide with plasma particles and transfer their kinetic energy. Lastly the particles are accelerated by introducing electromagnetic waves which heat the plasma in much the same way as a microwave oven heats food. Ultimately the products of the fusion reactions themselves will carry kinetic energy which is partially transferred to the plasma to maintain the temperature [6]. The never ending development of fusion reactors owes to a need for reactor upscaling, which provides new engineering challenges as new techniques must be developed in order to properly apply the lessons learned from previous experiments. The largest machine currently being built is the International Thermonuclear Experimental Reactor (ITER). This is an iteration of previous tokamak reactor designs, aiming to prove the scientific and technological viability of fusion power. The machine is designed to host a large volume of plasma, as the ratio of volume of reacting plasma to the ratio of surface heat losses is cubic versus squared [15]. This means that magnetic confinement fusion favours large machines, thus the ITER is a lot larger than its predecessors, and future designs will be even larger. The ITER will be the first fusion device to produce a substantial amount of usable energy as a proof of concept for future generations of Tokamaks.

Stellarator

The Stellarator is an alternative design to hold the high temperature plasma. This machine is able to maintain a constant operation as there are additional physical toroidal coils added to induce the poloidal magnetic field directly. Modern Stellarators actually use helical coils directly to produce the required magnetic field. Simulations of plasma behavior give the design parameters for the coils, which can be rather odd looking.

2.4.2 Inertial confinement fusion

Inertial confinement fusion technology aims to compress a pellet of fuel to a density at which nuclear fusion occurs. Fusion probability increases with decreasing distance between atoms, thus high temperature is not the only driver for fusion. Our sun is an example of this, where the enormous gravitational field produces high pressure enabling fusion at the relatively low temperature of 10,000,000 degrees Celsius [11]. Inertial confinement fusion aims to mimic this approach by compressing the gas instead of heating it. Using laser beams, gas is compressed to a density of 1000 g/cm³ or a tonne per liter [6] which is sufficient for fusion. There are two main approaches to inertial confinement fusion, direct drive and indirect-drive.

Direct drive

Direct drive uses lasers or ion beams to compress fuel adiabatically to a density where the atoms come close enough to fuse. The fuel is contained in a pellet with a shell that ablates easily. Upon laser or ion bombardment from all (or as many as possible) directions, the shell vaporizes and a shock-wave is sent inward to compress the fuel contained within the pellet to ignite fusion reactions. This method demands many powerful lasers or ion beams.

Indirect drive

Indirect drive is an alternative approach to achieve the desired radiation. By introducing a metal cylinder around the fuel pellet called the Hohlraum, lasers or ion beams directed at the cylinder top and bottom open surfaces fire in the mega joule range and immediately evaporate the metal, turning it into a plasma. This plasma releases a huge amount of x-rays, which then ablates the pellet shell, compressing the fuel to fusion conditions. The advantage of indirect drive is that the radiation hitting the fuel pellet is more isotropic, producing a higher quality spherically symmetrical implosion.

There are several setup variations for inertial confinement fusion, such as adding a small gold cone to direct the laser or applying a magnetic field to reduce electron thermal conductivity. Variations are being experimented with at multiple research facilities around the world, though the fundamental challenge of both magnetic- and inertial confinement fusion is that one needs to avoid instabilities and turbulences in the plasma. Inertial fusion suffers from mixing due to Rayleigh-Taylor instabilities, the type of spontaneous mixing that occurs in the contact boundary between two fluids of different density, here in the boundary between the ablator material and the fusion fuel. These instabilities tend to destroy the spherical symmetry of the collapsing pellet hindering sufficient density [6].

2.4.3 Z-pinch

Z-pinch is another technique being pursued in some research facilities. A large current is fired over a period of ~ 100 ns. through multiple wires set up in a cylinder shape which evaporates the wires leaving a plasma collapsing under its own magnetic field. High temperature plasma and a burst of X-rays converge toward the center axis, and by placing some deuterium as fuel on the axis, fusion has been achieved using this method. The current running through the wires in current experiments is about 18MA, and future commercial concepts aim for 70 MA currents [6].

2.5 Low temperature nuclear fusion processes

The only real obstacle to achieve nuclear fusion is the Coulomb barrier, which is overcome by bringing the particles close together. Kinetic energy through high temperature as known from magnetic- and inertial confinement is a direct and robust way to force the particles together, though it has proven very costly and require large machines to operate. Might there then be other methods available to achieve fusion?

2.5.1 Spontaneous fusion

Even though the interatomic distance in a molecule is small, the constituent nuclei do not readily fuse. The interatomic distances depend on the charge of the nuclei involved where more protons in a nucleus means more electrons can be bound. Molecular binding of atoms make use of the valence electrons which are in the outermost shell, furthest from the nucleus, resulting in the largest interatomic distances for atoms with many protons, while the smallest in molecules where the atoms have few protons.

A hydrogen molecule contain two protons and is stable at two distances depending on if it is bound by one or two electrons. Experiments have shown that the neutral hydrogen molecule is stable at 74 pm, while the hydrogen ion is stable at a larger distance of 105.7 pm. Deuterium bond length does not differ much from hydrogen and is also 74 pm as the same number of charges will produce the same electrical environment for bonding [16]. For these and all other known stable particles the probability of spontaneous fusion for all practical purposes is totally negligible.

An interesting hypothetical aspect on atoms fusing in a molecule was presented in 1989 when the two physicists Koonin and Nauenberg in a letter to Nature calculated the interatomic distance required to achieve the rate of fusion claimed by Fleischmann and Pons in [17]. By adjusting the electron mass which directly scales the nuclei separation distance, they found that a theoretical electron mass of $10m_e$ [18] would be sufficient to achieve the claimed rate of fusion. They concluded however that there was no current mechanism that would enable such distance enhancements. By scaling the interatomic distance of hydrogen this order of magnitude, 7.4 pm is the apparent upper fusion limit (UFL) distance according to Koonin and Nauenberg required for spontaneous deuterium fusion at low temperature. They also indicated that a factor of $5m_e$ would be sufficient to achieve the fusion rates claimed by a different group [19]. Another interesting comment they made was that a neutron free p+d reaction could play a role as they calculated it to have a significant probability, assuming that fusion actually did occur. This is an interesting aspect as some cold fusion experiments claim to observe no neutron radiation [20].

2.5.2 Spontaneous muon catalysed fusion

In this section spontaneous fusion due to formation of muon-bound exotic molecules is introduced.

Sir Frederick Charles Frank (1911 - 1998) and Andrei Dimitrevich Sakharov (1921 - 1989) both independently introduced the concept of muon catalyzed fusion in 1947 and 1948 respectively. In 1957, Luis W. Alvarez and others made the first experimental observation [21] of the phenomenon in a liquid hydrogen bubble chamber, where the group saw that muons which had come to a rest were re-ejected and re-energized. They concluded that what they saw was fusion of deuterium atoms. Research in this field has continued since and numerous experiments has confirmed the phenomenon [22].

The muon (μ^-) is an elementary particle similar to the electron but with 207 times more mass and a relatively short lifetime of $2 \mu s$. The muonic atom is two hundred times smaller than a regular atom with an electron orbital radius of $260 fm$. The muonic atom can bind to another nucleus, resulting in a muonic molecule about 207 times smaller than if bound with an electron. Nuclear fusion at these interatomic distances have a relatively high probability, though break-even where energy production is larger than energy consumption has so far not been achieved. After a muon has catalyzed a fusion reaction, it can bind to another hydrogen isotope and continue catalyzing reactions. During its lifetime, one muon can catalyze around 150 reactions. However as one of the products of fusion reactions is a helium nuclei, there is a slight chance (0.44%) that the muon will stick to this particle and eventually decay. If 300 reactions per muon with a 0.33% sticking rate could be achieved the process would reach energetic break-even, though this seems highly unlikely in the present understanding of the phenomenon [22].

2.6 So called ultra-dense deuterium

There are claims that scientists in Sweden are observing what they call ultra-dense deuterium $D(-1)$, which is said to be a set of tightly packed deuterium atoms. They claim to observe the state using a pulsed laser induced Coulomb explosion which results in an energy release of $630 \pm 30 eV$ corresponding to an interatomic distance D-D of $2.3 \pm 0.1 pm$ [23]. The notation of $D(-1)$ is based on an indication where comparing dense hydrogen materials to their inverted states result in the distance $2.5 pm$ [24].

Most of their experimental evidence is based on Time of Flight Mass Spectrometry (TOF-MS), where they measure velocities of particles believed to result from Coulomb explosions in ultra-dense deuterium. A Coulomb explosion is what happens when a chemically bound substance is stripped of its binding electrons enabling the positively charged nuclei to transform their repulsive potential energy into kinetic energy. By measuring the velocity of these particles, kinetic energy can be calculated and thus the initial potential energy. Coulombs law finally reveals the original distance between the charges since the potential energy is known.

In other experiments [25] by the same group, claimed laser-induced Coulomb explosions in ultra-dense deuterium $D(-1)$ show a broad spectrum of fragmentation processes. These experiments have shown particle energies up to $945 eV$, which would indicate even lower interatomic distances.

An attempt to describe how this so called ultra-dense deuterium can be stable has been made by Winterberg [26] where he claims different physical phenomena, such as Cooper pairs and Rydberg matter play a role. These mechanisms may play a role, however in providing a "clean" explanation they seem counterproductive. After studying previous work on ultra-dense deuterium, it seems that there is no real evidence for the existence of the $D(-1)$ matter, as the arguments appear to be

circular with references pointing only to the same type of experiments and hypothetical discussions.

The reports of experiments indicating short interatomic distances has motivated the theoretical study of this thesis. As the goal is to produce clear arguments, the circular reasoning presented by others is avoided and a completely different aggregate based only on quantum mechanical reasoning is suggested. Unlike the claims of the above authors we do not assume the existence of an unknown phase of matter, rather we explore a possibility that a cluster of nuclei might form a stable or a metastable system by a well known mechanism which is the basis of all molecular stability. Molecules are stable due to the quantal electronic states where binding energy of the electrons is somewhat larger than the Coulomb repulsion of the nuclei. Thus the argument is that the mechanism which explain regular molecules should also be able to indicate an eventual stable state of this ultra-compressed aggregate.

In an atomic cluster of high density which is the rough understanding of the state to be explored, multiple deuterium nuclei are clumped together at distances much shorter than the chemical distances in normal molecules. The shape of the Coulomb potential energy field exerted by each proton may then overlap due to small distances, resulting in a potential well which can host multiple deeply bound electrons. This could result in a stable or metastable configuration of such a cluster.

2.7 Relative distances

The above mentioned muonic molecule and suggested ultra-dense deuterium both have very small internuclear distances. Fig. 6 illustrate these distances in comparison to the more common Bohr radius and hydrogen molecule bond length. Also shown is the UFL distance discussed in section 2.5.1, which is the interatomic distance required to achieve the fusion rates claimed by Fleischmann and Pons.



Fig. 6: Approximate relative distances between two nuclei where zero and a red dot represent the two nuclei positions for Muonic molecule μ , ultra-dense deuterium $D(-1)$, Bohr radius a_0 (between proton and *electron* as red dot), hydrogen molecule H_2 and hydrogen molecule ion H_2^+ . Shown also is the upper fusion limit.

Units in Fig. 6 are not given, as the interesting concept is the relative distances included. As is seen, distance in the so called ultra-dense deuterium is smaller than the UFL, which means that if the state exists, nuclear fusion should be well within reach.

The suggested exotic aggregate immediately raises the questions whether or not such a state can be stable, and if so, how much energy does its creation require, what conditions are required, and will the state eventually be stable long enough to achieve nuclear fusion? This thesis only attempts to answer whether or not such an ultra-compressed state can be stable, meaning that only one of many questions will be investigated in the following chapters.

3 Quantum physics

This section covers the physical and mathematical operations needed to conduct a preliminary numerical assessment of ultra-compressed hydrogen clusters. Quantum chemistry provide tools to indicate the stability of an atom or a molecule by evaluating the interplay of forces exerted by protons and electrons.

3.1 Quantum Chemistry

The stability of molecules can be described through quantum chemistry. By evaluating the molecular Hamiltonian, the overall sum of key energy relations can be determined to express the stability of a molecule. The quantities which must be identified are the following:

1. Kinetic energy of electron
2. Kinetic energy of nucleus
3. Potential energy of electron
4. Potential energy of electron-electron repulsion
5. Potential energy of nucleus-nucleus repulsion

The evaluation is done by solving the so called time independent Schrödinger equation for the electron in a range of pre-determined nuclear setups. Once the energy levels for a specific setup are determined, the nuclei are rearranged to a neighboring setup and the process repeated. By repeating the process a number of times and logging nuclei setup, binding energy, and nuclear repulsive energy, one can determine eventual stable states for the molecule. The plot that shows the sum of energies versus internuclear distance is called the potential energy surface (PES) . If the system has a stable configuration, it will appear as a minimum on the PES plot. If there are multiple local minimums on the plot, the system is said to have so called metastable states. It is common to separate the evaluation into electronic and nuclear parts by the Born-Oppenheimer approximation. This approximation assumes that the nuclei are fixed in space thus providing the potential energy where the electrons may be bound. This approach simplifies the analysis as only the electron wave function must be evaluated for the varying configurations of the nuclei.

3.2 The Schrödinger equation

To understand how and why the Schrödinger equation is used in state analysis, bound electron behavior is briefly discussed. Protons in a nucleus produce a force field where electrons may be bound. Far away from the nucleus where electron movement is unrestricted, the electrons are said to be unbound. In 1924, Louise de Broglie observed that the electron, as well as any other particle, can be represented by waves. By studying wave mechanics, bound electrons proved to exist only in well defined discrete energy levels. These energies can be calculated using the Schrödinger equation. This equation plays the same role for quantum mechanics as Newtons equations of motion do for classical mechanics, and has been successfully used in countless applications. The full non-relativistic Schrödinger equation

$$H\Psi(\mathbf{r}, t) = i\hbar\frac{\partial}{\partial t}\Psi(\mathbf{r}, t) \quad (3.1)$$

contains the Hamiltonian operator H , also known as the energy operator, the imaginary number i , the reduced Planck constant \hbar , the time derivative $\frac{\partial}{\partial t}$ and the state $\Psi(\mathbf{r}, t)$ which is a function in space $\mathbf{r} = [x\mathbf{i}, y\mathbf{j}, z\mathbf{k}]$ and time t . On the left hand, the Hamiltonian operator represents the energy associated with the state, while the right hand side contains the temporal evolution of the state.

The Hamiltonian operator

$$H = T + V \quad (3.2)$$

contains the kinetic and potential energy operators T and V respectively. The kinetic energy operator

$$T = \frac{p \cdot p}{2m} \quad (3.3)$$

is given by the momentum operator p and particle mass m . The momentum operator

$$p = \frac{\hbar}{i} \nabla \quad (3.4)$$

contains the gradient operator ∇ , the reduced Planck constant \hbar and the imaginary number i . The gradient operator

$$\nabla = \frac{\partial}{\partial x} \mathbf{i} + \frac{\partial}{\partial y} \mathbf{j} + \frac{\partial}{\partial z} \mathbf{k} \quad (3.5)$$

finally takes the derivative with respect to all spatial coordinates. The potential energy operator

$$V = V(\mathbf{r}, t) \quad (3.6)$$

is the potential in spatial coordinate \mathbf{r} at time t .

The time-independent Schrödinger equation can be derived from equation 3.1. We search for solutions which can be written in separate spatial and temporal form, $\Psi(\mathbf{r}, t) = \psi(\mathbf{r})f(t)$. Eq. 3.1 then reads

$$H\psi(\mathbf{r})f(t) = i\hbar\psi(\mathbf{r})\frac{\partial}{\partial t}f(t) \quad (3.7)$$

By further separating the variables of spatial and temporal terms to either side,

$$H\psi(\mathbf{r})\frac{1}{\psi(\mathbf{r})} = \frac{i\hbar}{f(t)}\frac{\partial}{\partial t}f(t) \quad (3.8)$$

functions that solve the left side will be dependent only on \mathbf{r} , while the right side will depend only on t , both of which are independent variables. The only functions which satisfy this condition are constants, since both sides of the equation must be equal independent of input. Therefore the two sides can be separated into two equations. The constant is often denoted as E since the Hamiltonian operator is associated with energy. There can be multiple constants, called eigenvalues, which solve the separable linear differential equation, which means the general solution is the linear combination

$$\Psi(\mathbf{r}, t) = \sum_E \psi_E(\mathbf{r})f_E(t) \quad (3.9)$$

The right hand side of equation 3.8 reads

$$i\hbar\frac{\partial}{\partial t}f(t) = Ef(t) \quad (3.10)$$

and the left side containing the energy of the system now reads

$$H\psi(\mathbf{r}) = E\psi(\mathbf{r}) \quad (3.11)$$

This is the time-independent Schrödinger equation for finding the stationary state eigenvalues.

One-dimensional time independent Schrödinger equation

Rewriting Eq. (3.11) for a one dimensional system is a matter of algebraic substitution after modifying the expressions shown in table 1. The one dimensional time independent Schrödinger equation then reads

$$\left[-\frac{\hbar^2}{2m} \frac{d^2}{dx^2} + V(x) \right] \psi(x) = E\psi(x) \quad (3.12)$$

This equation is much like the Helmholtz equation for waves in classical mechanics, though with different operators acting on it.

Table 1: Equations for time independent, one dimensional system.

| Eq. ref | 3D, time dependent | 1D, time independent |
|---------|---|----------------------|
| (3.6) | $V(\mathbf{r}, t)$ | $V(x)$ |
| (3.5) | $\nabla = \frac{\partial}{\partial x} \mathbf{i} + \frac{\partial}{\partial y} \mathbf{j} + \frac{\partial}{\partial z} \mathbf{k}$ | $\frac{d}{dx}$ |

Atomic units

Treatment of units in quantum mechanics can be done in various ways. It is convenient for calculations to use units of simple values, preferably 1. This is often done by letting rest mass m_e , charge e and the reduced Planck's constant \hbar take the value 1. The Bohr radius

$$a_0 = \frac{\hbar^2}{m_e e^2}$$

then becomes 1 atomic unit of length. Units of energy also simplify, where $1 \text{ a.u.} = 27.2 \text{ eV}$, which is twice the ionization energy of the ground state electron in hydrogen. Atomic units conveniently simplifies the Schrödinger equation by eliminating some factors. Thus the one-dimensional time independent Schrödinger equation in atomic units finally reads

$$\left[-\frac{1}{2} \frac{d^2}{dx^2} + V(x) \right] \psi(x) = E\psi(x) \quad (3.13)$$

3.3 The wavefunction

The state $\psi(x)$ contains all information about observable properties of the particle, such as position and momentum. The discussion here is for a one dimensional time independent system where x is the spatial coordinate in one dimension, though the same concepts are also true in three dimensions and time. The function $|\psi(x)|^2$ is a position probability density distribution. Expectation value of specific properties is given by $\int \psi(x) A \psi(x) dx$, where A is an appropriate operator such as the Hamiltonian operator. Since the wave function squared represents the probability distribution of where to find a particle, there are some natural limitations to it.

It is necessary to assume that the probability of finding a bound electron outside the atomic radius approaches zero, which gives the boundary condition $\psi(x) \rightarrow 0$ for $x \rightarrow \infty$.

Another condition is that the probability of finding the particle within the area covered by the wave function squared must sum to absolute certainty, or 1.

$$\int_x |\psi(x)|^2 dx = 1 \quad (3.14)$$

Wave functions that meet this condition are called normalized. Non-normalized functions $\phi(x)$ can be normalized by letting $\psi(x) = C\phi(x)$, and substituting this into equation 3.14. The normalization constant C can then be solved for.

$$C = \left(\int_x |\phi(x)|^2 dx \right)^{-1/2} \quad (3.15)$$

The last criteria for the wave function is that it must be continuous and smooth.

Orthonormal functions

One method to obtain the wave function is to represent it as the linear sum of other functions. This is possible due to the theory of expansion in terms of a complete set of functions. Any function $g(x)$ on an interval $x \in [a, b]$ can be represented by a complete set of functions, or a basis set, $\{U_n(x)\}$ with appropriate constants $\{C_n\}$ where $n \rightarrow \infty$ and $n \in \mathbb{N}$ as

$$\sum_{n=1}^{\infty} C_n U_n(x) = g(x) \quad (3.16)$$

The formal definition is that

$$\lim_{n \rightarrow \infty} \int_a^b \left| g(x) - \sum_n C_n U_n(x) \right|^2 dx = 0 \quad (3.17)$$

which shows that the difference between the original function and the constructed one must approach zero for large n . If the so called inner product

$$\int_a^b U_j(x) U_k(x) dx = 0, \quad j \neq k \quad (3.18)$$

the functions $\{U_n(x)\}$ are said to be orthogonal. If the functions furthermore are *orthonormal*, the inner product becomes

$$\int_a^b U_j(x) U_k(x) dx = 1 = \delta_{jk}, \quad j = k \quad (3.19)$$

where δ_{jk} is called the Kronecker delta function. If $j \neq k$, the inner product is still zero. These are useful properties when solving the Schrödinger equation, as a specific coefficient C_j can be identified through

$$\int_a^b g(x) U_j(x) dx = \int_a^b \sum_{n=1}^n C_n U_n(x) U_j(x) dx = \sum_{n=1}^n C_n \delta_{nj} = C_j \quad (3.20)$$

It should be noted that when the functions are complex, it is necessary to use the complex conjugate $g^*(x)$ when calculating the inner product.

Hamiltonian operator

The Hamiltonian operator H modifies the wave equation to express information about the energy associated with it. It is an hermitian operator in the Hilbert space. Hilbert space is an abstract vector space with any number of dimensions. Hermetian operator eigenvalues are real and the eigenfunctions or eigenvectors are orthogonal. The eigenfunction(s) is any function Ψ , and the eigenvalue(s) any value E that satisfies $H\Psi = E\Psi$. If more than one eigenfunction correspond to a given eigenvalue, the eigenvalue is said to be degenerate. Degeneracy however do not appear in one-dimensional systems.

Electron repulsion

In the full description of atomic and molecular systems the electron repulsion must be taken into account. This repulsion is in principle analogous to the Coulomb repulsion between nuclei. However the following is the case for the present analysis: The wavefunctions of the electrons are extended over a large area and the probability density plays an effective role as a charge density. Thus the situation can be described as electron charges spread into a continuous charge distribution, completely delocalized. Consequently, the repulsion between the "electron clouds" is generally much weaker than the repulsion between point charges.

In descriptions of inner shell electrons of atoms with many protons (Z) the effect of electron-electron repulsion is generally more than Z -times weaker than the nucleus - electron interactions. As the present analysis aims only to establish the possibility of binding of the system the electron-electron interaction can safely be neglected [27].

4 Method for determining bound states

In this section quantum chemical theory is used to develop a method to indicate if the suggested aggregate can be stable. It is important to keep in mind that quantum mechanics are based on models. In a first approach such as the present, simplified models are often valuable to provide indications of what behavior might be expected. Based on such preliminary results, the model may be refined and developed to produce more precise results. The model suggested for this analysis treats the problem as a one-dimensional, time independent system with no external forces present.

4.1 Solving the Schrödinger equation

Based on the theory presented in section 3, the one-dimensional time independent Schrödinger equation can now be solved to identify the states of a given system and the energies associated with them. In the space $x = [0, L]$ the wave equation can be represented through a complete set of functions

$$\psi(x) = \sum_n C_n \Phi_n(x) \quad (4.1)$$

where $\Phi_n(x)$ is chosen as the orthonormal set of functions

$$\Phi = \left\{ \sqrt{\frac{2}{L}} \sin\left(n \frac{\pi}{L} x\right) \right\} \quad (4.2)$$

normalized by the constant $\sqrt{\frac{2}{L}}$. The chosen functions meet the requirements of the wave function since $\Phi(0) = \Phi(L) = 0$ and the functions are continuous and smooth, however normalization must also apply to the coefficients

$$\sum_n |C_n|^2 = 1 \quad (4.3)$$

Eq. 4.1 can be substituted into 3.11 to give

$$H \sum_n C_n \Phi_n(x) = E \sum_n C_n \Phi_n(x) \quad (4.4)$$

By first multiplying each side with a specific state $\Phi_j(x)$ then integrating each side over the defined area, the associated energy C_j can be evaluated since

$$\int_0^L \Phi_j^*(x) H \sum_n C_n \Phi_n(x) dx = E \int_0^L \Phi_j^*(x) \sum_n C_n \Phi_n(x) dx = E \sum_n C_n \delta_{nj} \quad (4.5)$$

$$EC_j = \sum_n C_n \int_0^L \Phi_j^*(x) H \Phi_n(x) dx \quad (4.6)$$

where $\int_0^L \Phi_j^*(x) H \Phi_n(x) dx$ is recognized as the energy expectation value. Substituting $H = -\frac{1}{2} \frac{d^2}{dx^2} + V(x)$ into the above gives

$$EC_j = \sum_n C_n \int_0^L \Phi_j^*(x) \left[-\frac{1}{2} \frac{d^2}{dx^2} \right] \Phi_n(x) dx + \sum_n C_n \int_0^L \Phi_j^*(x) V(x) \Phi_n(x) dx \quad (4.7)$$

where the kinetic energy can be written as

$$\sum_{n=1}^n C_n \int_0^L \Phi_j^*(x) \left[-\frac{1}{2} \frac{d^2}{dx^2} \right] \Phi_n^*(x) dx = \sum_n C_n T_n \int_0^L \Phi_j(x) \Phi_n(x) dx = T_j C_j \quad (4.8)$$

where $T_j = \frac{1}{2} \left(\frac{n\pi}{L} \right)^2$ for this set of functions. The potential energy term includes the potential operator $V(x)$ which is the main manual input to the analysis. The complete equation finally reads

$$T_j C_j + \sum_n C_n \int_0^L \Phi_j^*(x) V(x) \Phi_n(x) dx = E C_j \quad (4.9)$$

where C_j is governed by the Kronecker delta function only taking on values for $j = n$, which can be represented as a column vector. By arranging Eq. 4.9 in square $n \times n$ matrices

$$\begin{bmatrix} T_{11} & 0 & \dots & 0 \\ 0 & T_{22} & \dots & 0 \\ \dots & \dots & \dots & \dots \\ 0 & 0 & \dots & T_{nn} \end{bmatrix} \begin{bmatrix} C_1 \\ C_2 \\ \cdot \\ C_n \end{bmatrix} + \begin{bmatrix} V_{11} & V_{12} & \dots & V_{1n} \\ V_{21} & V_{22} & \dots & V_{2n} \\ \dots & \dots & \dots & \dots \\ V_{n1} & V_{n2} & \dots & V_{nn} \end{bmatrix} \begin{bmatrix} C_1 \\ C_2 \\ \cdot \\ C_n \end{bmatrix} = E \begin{bmatrix} C_1 \\ C_2 \\ \cdot \\ C_n \end{bmatrix} \quad (4.10)$$

every state and its corresponding energy is retrievable. Every element in the potential energy matrix evaluate the expectation value $V_{jn} = \int \Phi_j^*(x) V(x) \Phi_n(x) dx$. Eq. (4.10) is an eigenvalue problem on the form $(A + B)V = \Lambda V$, where Λ is the eigenvalue matrix and V eigenvectors. The eigenvalue matrix is retrieved by diagonalizing $V^{-1}(A + B)V = \Lambda$. The eigenvalues are the diagonal entries of Λ . The state function corresponding to E_{jn} is retrievable by scaling the eigenvector with a row vector consisting of the basis functions.

The eigenvalues represent the binding energy of the electrons, where bound states have negative values. Every state can be occupied by two electrons and the total number of electrons cannot exceed the total number of protons.

4.2 Nuclei arrangement and repulsion

The theory presented in previous section allows the binding energy of the electrons to be calculated. Now the repulsive energy between the nuclei must be established to determine if stable states can exist. The electric repulsive potential energy U in units of Joules is given by integrating the electric force given in equation 2.2 from infinite separation to the final separation distance

$$U = \int_{\infty}^d F_e dr = k_e \frac{q_1 q_2}{d} \quad (4.11)$$

where k_e is the Coulomb constant, q_1 and q_2 the charges of the system, and d the distance between them. In a system of like single charges $q_1 q_2 = e^2$. In atomic units, both the Coulomb constant k_e and the elementary charge e take value 1. Eq 4.11 in atomic units then becomes simply $1/d$ for single charged nuclei. When a system consists of more than two charges, the energy between every pair is first calculated before taking the algebraic sum to represent the total repulsive potential energy. The position of each charge effects the repulsion. For example, four protons clumped together in a tetrahedral configuration will have the same distance between all charges $d = 1 \text{ a.u.}$, producing $6 \times 1/1 = 6 \text{ a.u.}$ of repulsion through the sum of six pairs. However, if the four protons are arranged in a straight line as shown in Fig. 7, the potential energy is minimized. If each proton is separated from the next by distance $d = 1 \text{ a.u.}$, the repulsion would be less as a consequence of varying distances in the pairs. There would still be six pairs of interacting charges, though only three at $d = 1$, two at $d = 2$ and one at $d = 3 \text{ a.u.}$ The resulting repulsion of the string evaluates as the sum $3/1 + 2/2 + 1/3 = 4,33 \text{ a.u.}$ of repulsive energy.

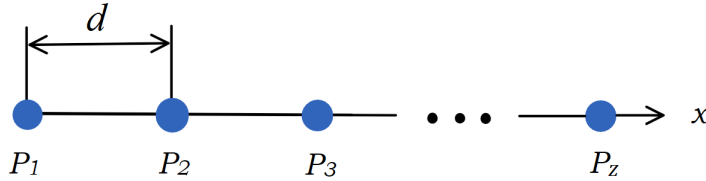


Fig. 7: Nuclei positioning.

The expression for repulsive energy in atomic units of z single charge nuclei aligned on an axis has been found to be

$$U = \frac{1}{d} \left(z \sum_{k=1}^{z-1} \frac{1}{k} - (z-1) \right) \quad (4.12)$$

the derivation of which can be found in appendix A.

4.3 Potential energy felt by electrons

The system to be analyzed consists of equidistant single charge nuclei positioned as shown in Fig. 7, aligned on an axis since this is shown to minimize repulsion. Number of nuclei and the distance between them are the main variables, with one elementary charge per nucleus held constant. The model will analyze the behaviour of a finite but varying number of nuclei at different distances in search of stable states. The potential $V(x)$ is given as the sum of Coulomb potential contributions from each nuclei at coordinate \mathbf{P}_z along the axis:

$$V(x) = - \sum_z \frac{1}{|x - \mathbf{P}_z|} \quad (4.13)$$

The distance between any two neighbouring nuclei is modified by the distance factor d , where $d = 1$ indicates the Bohr radius 1 *a.u.* of length between two nuclei. The potential introduces singularities

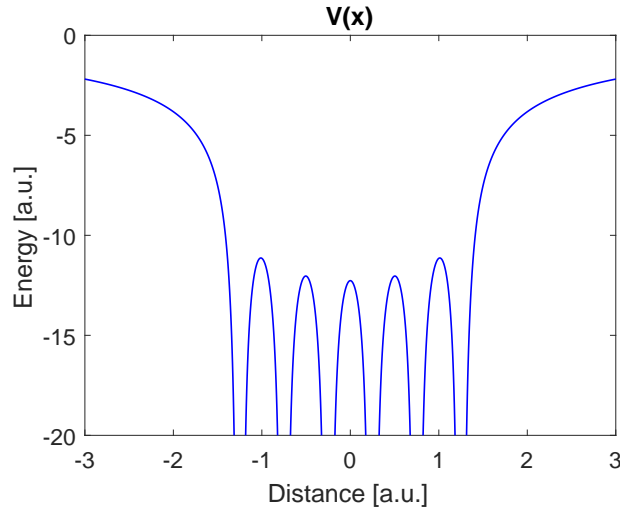


Fig. 8: One dimensional potential for 6 nuclei with infinite negative potential at each nuclei.

at every $\mathbf{P}_z = \mathbf{x}$, as shown in Fig. 8 which cannot be solved in the Schrödinger equation due to the need of integrating the potential which is infinite in the one-dimensional case. Therefore modification of the potential to remove the discontinuities is needed before the system can be analyzed through the Schrödinger equation.

If the potential was evaluated in three dimensions, the potential integral would converge with no correction needed as integrating includes multiplying by r^2 :

$$\int \frac{1}{r} r^2 dr = \frac{r^2}{2} \quad (4.14)$$

Solving the Schrödinger equation in three dimensions is a much more complicated task which has not been attempted in this work, however due to rotational symmetry along the axis cylindrical coordinates could be used to simplify the task. The potential has nevertheless been created in all three dimensions to illustrate the system. Two-dimensional potential is shown in Fig. 9 and three dimensional is shown in Fig. 10, where it can be seen that the potential becomes spherical at a distance.

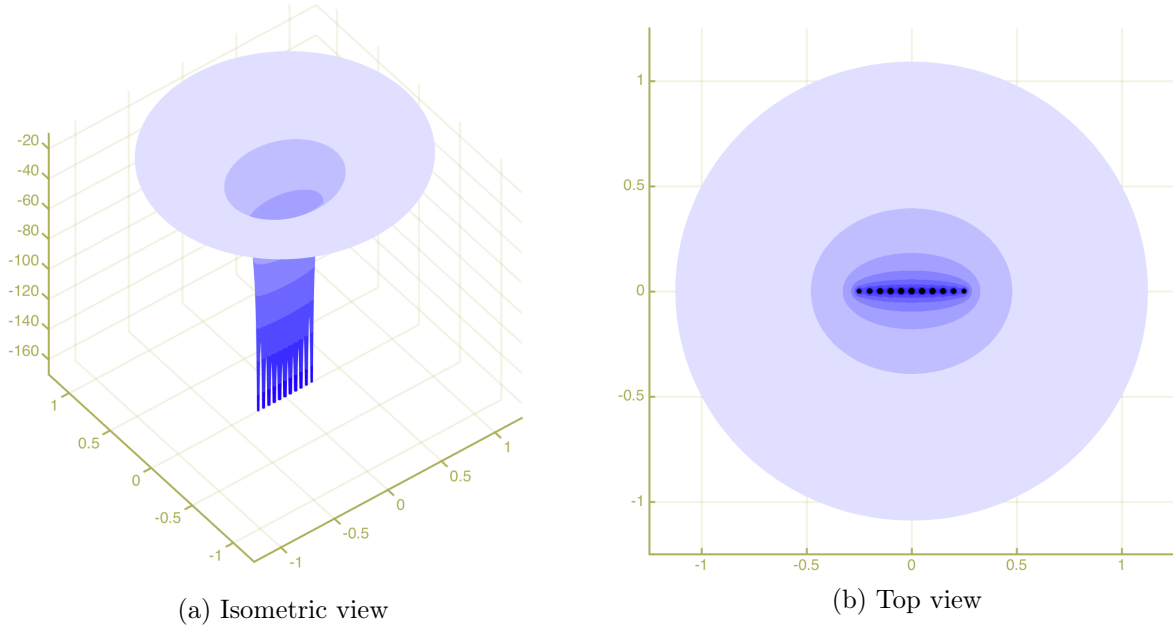


Fig. 9: Two dimensional potential plot for 11 nuclei at distance $0.05a.u.$, z axis shows energy as function of x and y.

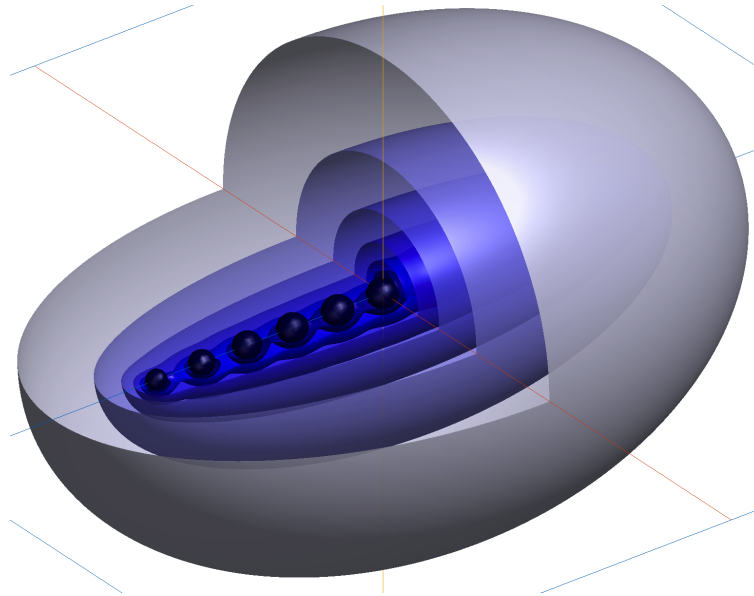


Fig. 10: Three dimensional iso-surface potential plot for 11 nuclei at distance $0.05 a.u.$, iso-surfaces shown for energy values -10 to -80 in steps of $10 a.u.$.

4.3.1 Potential terminology

In further discussions about the potentials, some terminology as presented in Fig. 11 will be convenient to introduce. The shape resembles a potential well, where what is referred to as the bottom is limited by local potential maximums between any two neighbouring nuclei. At each nucleus the potential stretches down into infinity, referred to as "hair". All local maximums when connected form a "u" shaped bottom. The lowest local maximum is the bottom potential V_b . The energy difference between the highest and lowest local maximums is ΔV_{well} .

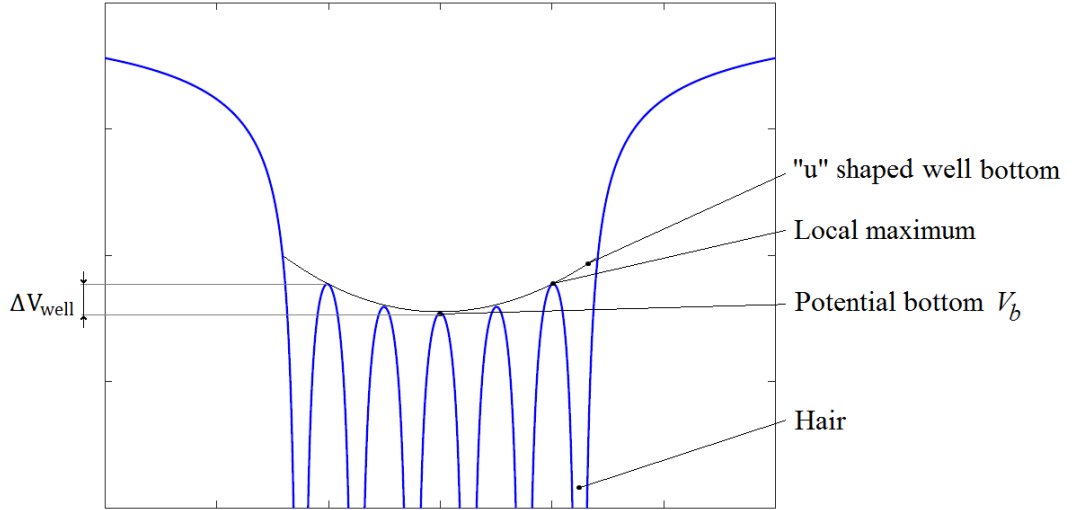


Fig. 11: Figure shows terminology for potential. Axis are same as in Fig. 8

4.3.2 Soft Coulomb potential

By applying a softening term b to the potential, the function is approximated without infinity discontinuities as follows:

$$V(x) = - \sum_z \frac{1}{(\sqrt{|P_z - x|}^2 + b)} \quad (4.15)$$

The effect of this softening is shown in Fig. 12, where the solid and stippled lines represent the

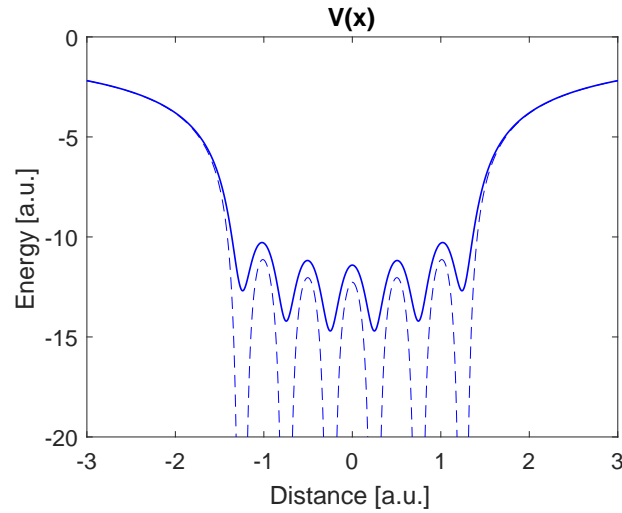


Fig. 12: Softened Coulomb potential example.

softened and original Coulomb potentials respectively. Usually the parameter b can be calibrated to produce a sensible potential, although for this application the potential is significantly modified over a wide range and not only at the discontinuities as shown in Fig. 12, which makes the method unusable for this analysis. Soft Coulomb potentials have been successfully used by others [28] [29], but mainly for single point charges where the potential is less complex.

4.3.3 Truncated Coulomb potential

A truncated Coulomb potential is one where the potential is left unchanged except around the discontinuities by $V(x) = V_{cut}$ for $V(x) \leq V_{cut}$. This way of limiting the discontinuities does not affect the shape of the potential where unintended, which makes the method favorable for this analysis. The method provides a lower limit for the potential at chosen value V_{cut} . By varying the depth of the potential cut, it is observed that when solving for eigenvalues the binding energy of the electrons is directly influenced, where a deeper potential cut result in higher electron binding energies. This is in agreement with other reports on truncated Coulomb potential [30]. By evaluating some boundary conditions on what energies are expected, reasonable potential cut depths have been found and applied in the analysis.

As distance between nuclei approach zero, binding energy of the electrons must eventually resemble that of the atom with the same number of positive charges in its nucleus. The ground state electron for any atom has binding energy $E_0 = -\frac{1}{2}Z^2$ in atomic units. Therefore, as $d \rightarrow 0$, the program should produce a ground state eigenvalue approaching E_0 . Such a program has been developed which calculates and logs required cut depth to reproduce E_0 for atoms with a range of protons. By transferring these V_{cut} values to the string potential, the ground state eigenvalue approaching E_0 as $d \rightarrow 0$ is generated. An example is shown in Fig. 13 where the cut depth results in the ground state for Calcium.

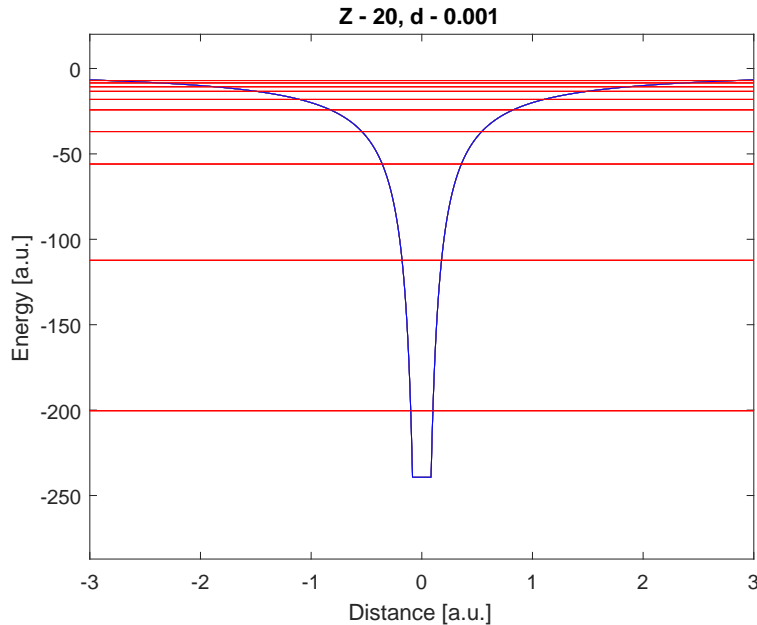


Fig. 13: Eigenvalues for small distance 0.001 *a.u.* When V_{cut} is set to -239 *a.u.*, the resulting first eigenvalue is -200 *a.u.*, which is the ground state energy E_0 for Calcium ($Z = 20$).

As distance increases from zero, the well bottom V_b eventually rises above V_{cut} as shown in Fig. 14, which acts as another limitation that pushes the eigenstates to lower energies. If the same V_{cut} continues to be the only limiting factor as d increases, the "hair" below the potential well bottom becomes thin and long. When eigenvalues are solved for in these cases, the first energy levels lie below the potential well bottom. It is possible that the eigenvalues should lie below V_b , however in one dimension it is difficult to determine what depth is realistic, as this is largely decided by the chosen potential cut depth. Instead of trying to identify the one correct cut depth, two extremes and one middle condition have been chosen to produce a solution space. The first

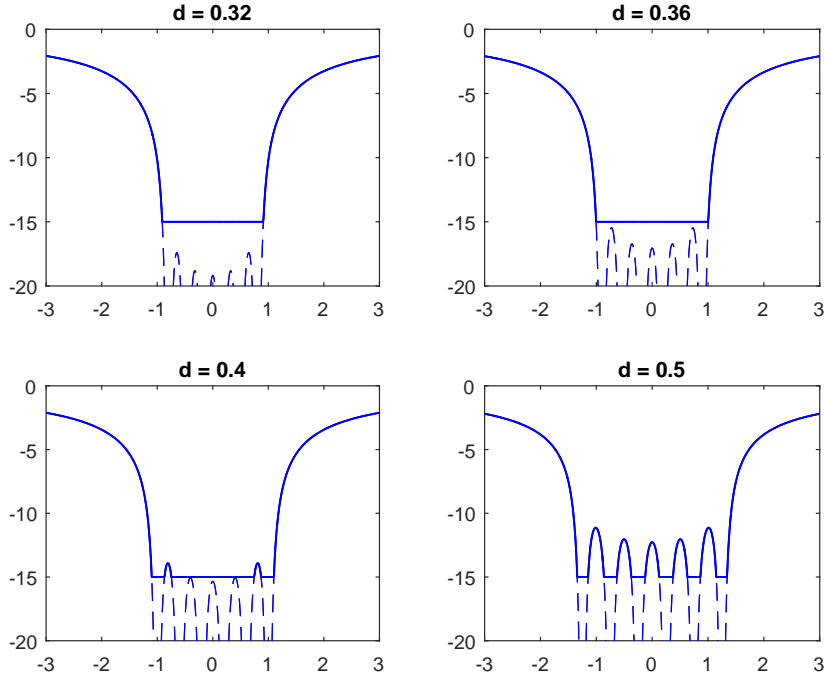


Fig. 14: Example of potential evolution where potential well bottom rises through potential cut (current cut depth is chosen only for illustration purpose). X and y axis are distance and energy a.u. respectively.

extreme condition is the most energetically conservative, which cuts the potential at V_b , producing relatively weak binding energies shown in Fig. 15, right side. The second extreme scenario yield radical binding energies by limiting the potential only at V_{cut} , shown in Fig. 15 left side. The third condition cuts the potential at V_{mid} , at a distance below V_b , shown in Fig. 15 middle. The distance in the V_{mid} mode is chosen so there is a proportional amount of "hair" always present under the well bottom, achieved as following: The energy span of the "u" shape, from the upper local maximum to the well bottom, is subtracted from V_b . This new depth is $V_{mid} = V_b - \Delta V_{well}$, chosen because it allows the eigenvalues to fall slightly below the well bottom.

4.4 Numerical tools

Matlab has been used to carry out all calculations in the analysis. Some relevant script files and functions can be found in appendix B, however the list is not exhaustive as some exploration programs have been omitted as they do not directly contribute to the results.

The Matlab codes and the one-dimensional model used here are an extension and specialization of a code used by the Atomic Physics Group project on atoms in strong electromagnetic fields published as [31], provided by J.P. Hansen and L. Kocbach.

Matlab cannot solve an $n \times n$ matrix where $n \rightarrow \infty$ as prescribed in Eq. 3.16, so a finite number which produces sufficiently accurate results must be used. By setting different values for n and running the program, minimum value for n was found when changes to the results were negligible if n was increased. If n is too small, the wave function does not completely decay outside the potential, but stays oscillating as not enough functions are summed. By setting $n = 400$, no oscillation was seen in any variable setup.

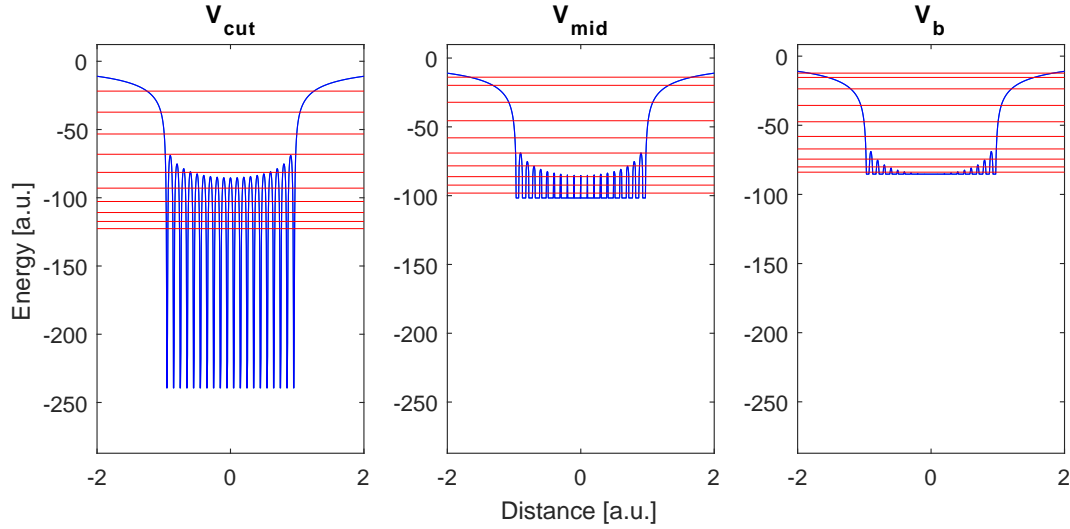


Fig. 15: Three different cut modes shown at distance 0.1 a.u. for 20 nuclei. V_{cut} result in eigenstates deep below potential well bottom, V_{mid} results in eigenstates slightly below well bottom and V_b result in eigenstates all above well bottom.

Program execution

During development of the different codes, a variety of programs were developed, tested, and improved upon. After satisfactory results were accomplished one major program to run through all necessary scripts and functions for all variable combinations was made. The list below names and briefly explains the main codes used to produce the results.

- Numerical Schrödinger equation script (appendix B.1) produces eigenvalues (binding energy) and eigenstates (wavefunctions).
- Truncation value optimization program (appendix B.2) establish truncation values producing ground state eigenvalues for very small distances equal to the united atom with same number of protons.
- Potential function (appendix B.3) produce one of three potentials based on what truncation mode is used. The program extracts truncation values from the results produced in the truncation optimization program.
- Repulsion script (appendix B.4) calculates repulsive energy of the string.
- Main analysis program (appendix B.5) runs all necessary scripts for the desired range of variables. Relevant results are then saved and plotted.
- Extra codes not in appendix: Two and three dimensional potential, search for potential scaling laws, string and single point potentials for comparison.

5 Results

A one-dimensional system of aligned equidistant single charged nuclei has been electronically analyzed in search of stable states. The variables are number of nuclei, distance between them and the truncation cut depth of the potential.

For different numbers of nuclei and three truncation methods, the Schrödinger equation has been solved for a variety of distances. The results have been logged and plotted to produce potential energy surfaces (PES). Each PES is constructed by solving the Schrödinger equation for a range of distances while number of nuclei and cut-off method is fixed. Thus three PES are constructed for a fixed number of nuclei, one for each cut-off method. An eventual minimum value on the PES indicate a stable state and the distance where this minimum occurs can be extracted. Minimum values for all combinations of variables have been extracted and compared to find lowest number of nuclei which stabilize at lowest possible distance. The results are shown in Fig. 16, where it can be seen that minimum distance increase with fewer nuclei, but seems to stabilize at around 15 nuclei and above depending on potential cut method.

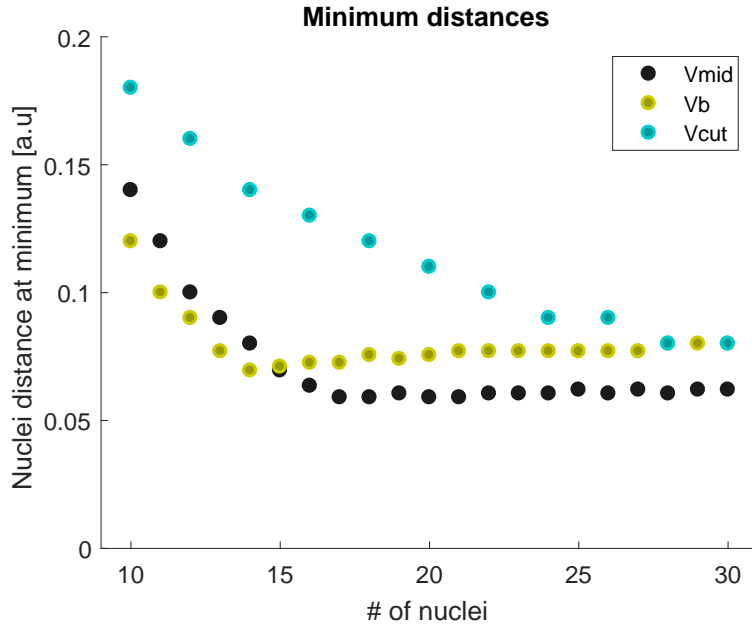


Fig. 16: Minimum distances for three potential truncation modes.

As Fig. 16 shows, the optimal conditions are located at 17 nuclei with cut-off method V_{mid} . The PES representing this situation is presented in Fig. 17, where the minimum occurs at distance 0.059 *a.u.* Fig. 18 shows the single analysis including wavefunctions representing the optimal variable configuration.

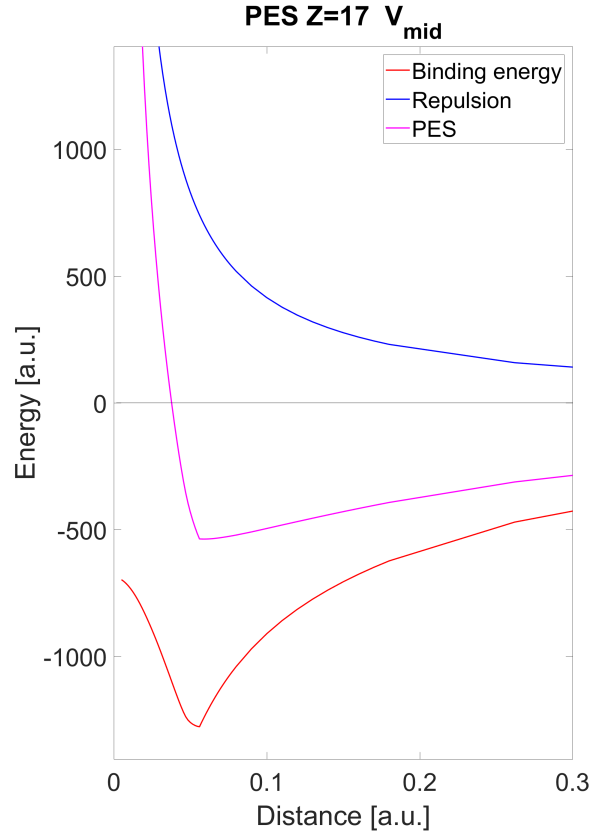


Fig. 17: PES for 17 nuclei with V_{mid} potential cutoff depth. Minimum is located at distance 0.059 *a.u.*

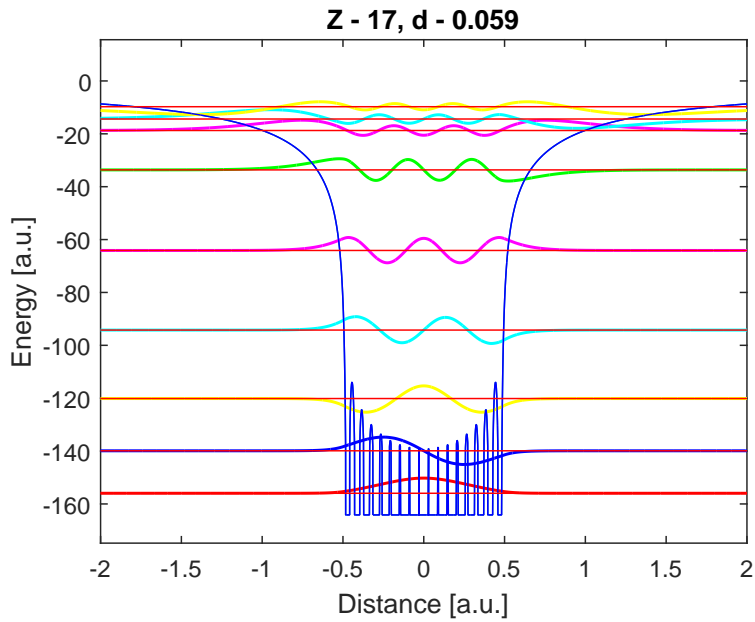


Fig. 18: Optimal configuration at $Z = 17$ and $d = 0.059$ using V_{mid} truncation.

6 Discussion

The idea that the suggested ultra-compressed aggregate may be composed of nuclei on a string comes from a simple observation that the total repulsion inside a string does not grow with Z^2 , so that the quantum binding could grow possibly faster. The results are rather unexpected but fully possible on the basis of known quantum chemistry; a molecule-like aggregate of multiple hydrogen nuclei arranged linearly, where equal numbers of electrons and protons are bound due to deep electron binding outweighing the nuclear repulsion in precisely the same manner as in any ordinary molecule.

The analysis has shown that minimums may exist at a high density axial nuclear configuration. However the inherent limitations of a one-dimensional model must be considered. The one-dimensional point charge Coulomb potential produces discontinuities at each nuclei which had to be removed before simulation. This was done by truncating the potential, which in this case meant to cut the potential at a chosen depth. Three rules were used to decide where to cut the potential, called the (three) truncation modes. The results show dependency on these as can be seen in Fig. 16. By using V_{cut} truncation mode, the minimum distances are generally larger than when using the two other modes due to the stronger bindings at larger distances when using V_{cut} . By comparing the two PES produced by V_{cut} and V_{mid} , as done in Fig. 19, the reason for the larger minimum distance using V_{cut} can be clarified. In V_{cut} truncation mode, the potential cut is maintained as V_{cut} throughout the analysis, meaning that the eigenvalues can sink far below the well bottom resulting in possibly unrealistically strong bindings. The two other truncation modes cut the potential at the well bottom (V_b) or near to it V_{mid} , which limits the binding energies of these modes. Notably, the differences are only present at distances where the potential well bottom is above V_{cut} , which can be seen in Fig. 19 for distances above ≈ 0.05 *a.u.* At smaller distances where the well bottoms are below V_{cut} , the binding energies for all three cut modes are identical since the potential must be limited by V_{cut} as $d \rightarrow 0$ to produce energies similar to the united atom with same number of charged protons in its nuclei. The reason why the binding energy initially increases as distance increases from zero, is because the potential well width naturally increases with d while the depth is maintained by V_{cut} , which allows for more deeply bound electrons with less energy difference between each state, seen as the eigenvalues "sinking" deeper into the well.

The analysis has been limited to distances up to 0.3 *a.u.*, because this is the area of interest. Distances up to 1.2 *a.u.* have been attempted analysed, showing a continuation of the energies seen in Fig. 19 where all energies gradually approach zero. This implies that any system of aligned single-charged nuclei should quickly stabilize at the small distances (≈ 0.06 *a.u.*) found. We know however that this does not happen because hydrogen isotopes are not normally observed in this state. Therefore results at distances larger than roughly 0.4 *a.u.* and above can not be correct. This regime of interatomic distances has not been studied further as it is larger than the scale of interest for this analysis. In any case there must be a mechanism that stops nuclei from naturally stabilizing at ≈ 0.06 *a.u.* A possible explanation is that at large distances the potential between each nuclei becomes very small, nearly removing the well shape of the potential which would allow localized electrons at each nucleus as in normal molecules. What is shown here is that each electron is delocalized and covers all the nuclei at these small distances. The need for a transition step, an event where the electrons at each atom must be ionized before a collapse into an ultra-compressed state, might act like a barrier stopping the nuclei from approaching each other beyond that of regular atomic distances.

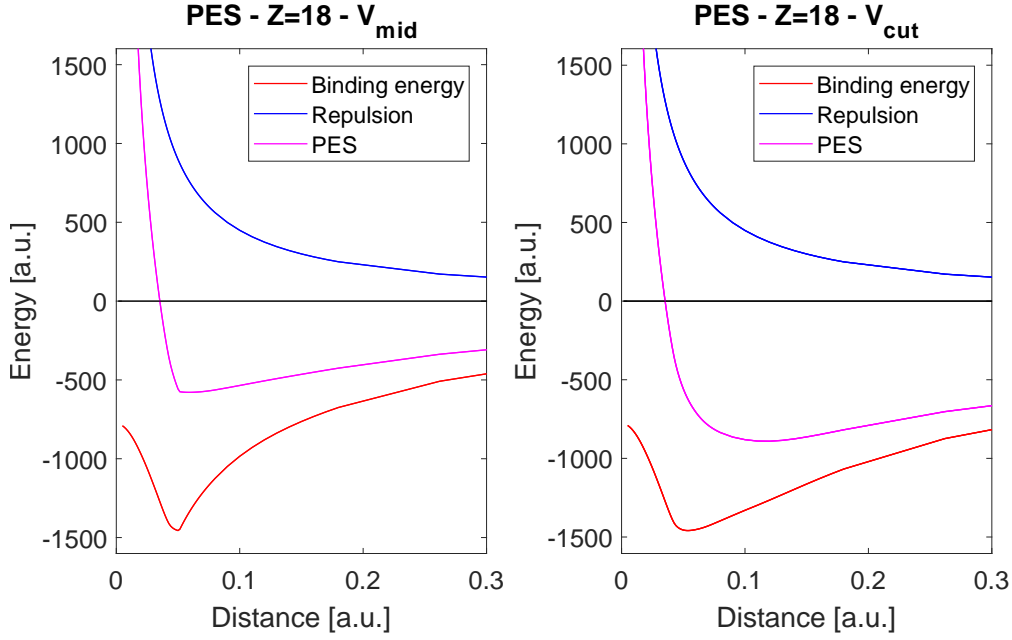


Fig. 19: PES comparison of truncation modes V_{mid} and V_{cut} . Stronger binding shifts the minimum to larger distance due to deeper potentials using V_{cut} .

By representing the wave function as a complete set of functions $\sum_{n=1}^{\infty} C_n U_n(x) = g(x)$, some information is lost since numerical simulations limit the number of functions in the sum. Another approach would be to search for the analytic function. This would increase the solution accuracy, though the benefit could be marginal as a more profound source of error is in the infinite potential at each nuclei. Also the number of functions of the sum has been varied and tested to ensure that this does not effect the results to any notable degree. In one dimension the number of functions needed is not too large, and around 400 has been found to produce satisfactory results. In three dimensions, this number would quickly increase to around 10 000 or more, where diagonalising a 10 000x10 000 matrix eventually becomes very time consuming, leading to resolution limitations.

Delocalised electrons

The wavefunctions that meet the boundary conditions are sums of eigenstates. For varying nuclei separation distances, the wavefunctions take on different shapes. Smaller distances produce smooth wavefunctions which look unaffected by the individual hairs of the potential, representing delocalised electrons. Larger distances produce dents in the wave, to the point where the wave is more localized at each nuclei and diminishes between them. The effect is shown in Fig. 20. At large distances, as the potential approaches zero between each nuclei, the system looks more like Bloch states in solids where there would be one (or two) electron located at each nucleus.

Is this cold fusion?

The results have indicated that there may exist a matter aggregate where the interatomic distance is $0.059 a.u.$. By conversion as $1 a.u. = 52.9 pm$, the calculated minimum distance is $3.1 pm$. As mentioned in section 2.6, the target distance of so called ultra-dense deuterium is $2.3 \pm 0.1 pm$. The results here show a distance somewhat greater than this, but within the same order of magnitude, deviations perhaps due to model weaknesses. This distance with regards to nuclear fusion probability

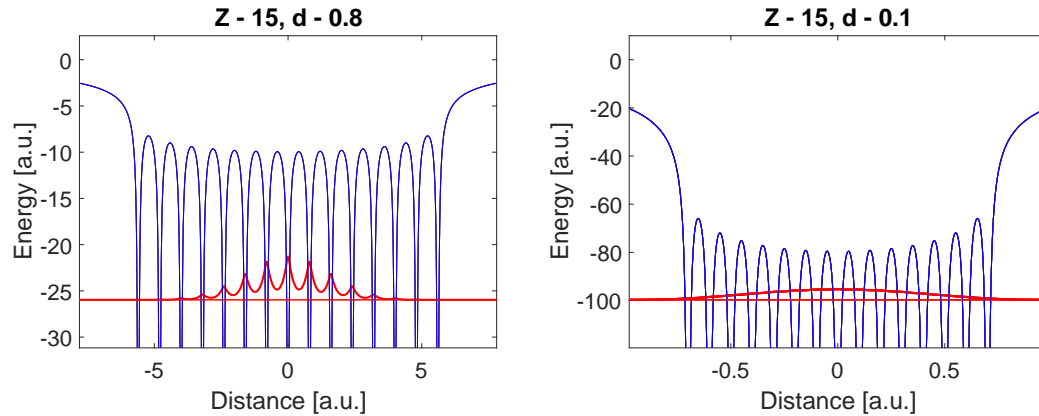


Fig. 20: Distance between nuclei affect the shape of the wavefunction, where large distances produce wavefunctions with localized peaks at each nuclei. At smaller distances the electron is mostly unaffected by each nuclei contribution as the space available is small. Blue lines represent potential, bold red line represent wave function and red line represents electron binding energy.

is very motivating as the theoretical upper distance limit presented in 2.7 shows that 7.4 pm or below could be sufficient to achieve nuclear fusion reactions. Based on this it is apparently possible that the discovered state can serve as the physical mechanism needed to explain claims of cold fusion as far back as 1989 although, considering the limitations of the current one-dimensional model and the possible implications of claiming this as a mechanism for cold fusion, detailed three-dimensional analyses should be performed before any such claims are made.

Program development

Initially the one dimensional model was expected to be based on the "soft Coulomb potential" which has previously been used in the Atomic Physics Group project [27] and was how the potential was formulated in the initial Schrödinger equation program I was given. It took some time before I understood that this would not work and learned about the alternative truncated Coulomb potential model. This gave me understanding of how theoretical physicists work, but experimenting with the unusable model cost quite a lot of work.

I learned early that the one-dimensional hydrogen atom does not work without removal of the singularity, and during my work I have understood the reason for this, as discussed in the potential energy section 4.3. Because of the necessity of truncation the model becomes less determined. Ideally the solutions should not depend on the way of the truncation. This is unfortunately not the case as is well known from the applications of such simple models in atomic physics. It was necessary to explore many different settings when trying to answer the question how to make the results reliable. Only the final solution is described in the text; the work leading to this final formulation has not been reported here as the text would become too long and after all, the unsuccessful trials are not of much interest. Nevertheless, it should be mentioned that the presented approach is a result of a significantly wider exploration.

A question might then arise why not use a three dimensional model which does not have any such problems. The main reason is that there was no readily available existing computer program for this model, and also the numerical and mathematical formulation is much more complex. Additionally the simple one-dimensional problem provides a clear understanding of the origin of the state, which is that the character of the potential changes from "Coulomb-like" to "potential well-like".

Thus a proper study and understanding of the one-dimensional case was judged by us more valuable than uncertain results of an untested three-dimensional model, a project which would be more suitable for a student specializing in theoretical physics. It seems however that the presented results will indeed lead to such an investigation of the three dimensional case by the Bergen Atomic Physics Group [27].

Creating the state

Creation of the state has not been analyzed in this thesis in any depth as the main focus has been to solely evaluate the stability of the proposed state. When looking at the system setup and by observing the resulting wavefunctions, some thoughts and discussions have nevertheless occurred. It seems that all nuclei must be ionized and then brought close together before the tightly bound state can be created. This because the electrons are spread out across the whole string and not one at each nucleus. Aligning the atoms to minimize repulsion might be achieved by having them absorbed along a dislocation in a crystal lattice.

It has been claimed that the state is stable before laser irradiation [32], which would imply spontaneous formation of the state. It seems more plausible to assume that such unusual systems can be a result of the energy brought by a laser pulse into a medium with large concentration of normal deuterium atoms in the bulk or surface of metallic host crystals.

Through discussions with members of the Bergen Physics Group [27], following thoughts on experimental creation of the ultra-compressed state have been made: A possible process could be that if a cluster of hydrogen atoms were exposed to extreme local pressures like those in a collapsing crystal lattice, the atoms could become effectively ionized, i.e. the nuclei would lose contact with their respective electrons. When surrounded by a metal lattice, these electrons would not be ejected as they could be absorbed as metallic electrons of the surrounding matrix. The bonding electronic states studied in this work would then be empty, and the formation of the state could be accomplished if these states were filled by electrons required to "jump down" emitting radiation. However, I have been told that radiative "recombination" is a relatively slow process and that perhaps tunneling from the inner shells of the atoms of the surrounding solid matrix could be a faster process. In any case, such events would be very rare under random conditions and without optimization the reproducibility would probably be limited.

If future full scale theory would fully confirm some type of stability of the proposed aggregates, simulations of possible formation scenarios could then help to search for and design arrangements of the metal matrix and eventual energy stimulation which could optimize or enable the process.

7 Conclusion and future perspectives

Nuclear fusion is a process able to produce vast amounts of energy, though currently the energy gain is less than the energy required to initiate the process. Much work is being done globally to achieve break-even, where the magnetic confinement and the inertial confinement approaches appear to be making the most progress. Experiments on so called ultra-dense deuterium have suggested another approach that might make possible low temperature fusion by bringing the nuclei to a small interatomic distance where they are claimed to be stable. The issue addressed in this work has been to explore the possibility of ultra-compressed deuterium clusters through quantum chemistry, as it appears that this kind of analysis has not been conducted previously.

This work should be viewed as a preliminary analysis, where it has been discovered that ultra-compressed hydrogen or deuterium clusters may exist as a state of aligned nuclei stable at an interatomic distance much smaller than seen in regular molecules. The equilibrium distance varies with number of nuclei in the string, where 17 nuclei seems to be the optimal number. The distance discovered is slightly larger than what the reported experiments on ultra-dense deuterium indicated. This might be a consequence of working with a one-dimensional model where manipulation of some parameters has been necessary to carry out the analysis.

The results are quite unexpected and if correct could mean a major theoretical breakthrough in the field of cold fusion/LENR. This is why attempts to reproduce these results in more rigorous models should be made, where as many aspects as possible are taken into account to discover flaws and missteps made in this work. If future analyses support the possibility that these aggregates can exist, more work on how they can be created is needed and experiments to test the theory should be conducted. Even if the discussed aggregates would not be suitable for energy production, establishing their existence itself should be of substantial scientific interest.

If such aggregates could be produced and optimized for energy expenditure, the impact on fusion based energy production could be of great importance. Rising global energy demand and global warming has convinced the IEA to encourage developed countries to focus on break-through energy technology research and development. This argument can be used to motivate further research on ultra-compressed hydrogen clusters, considering how unexplored this field of research is and the possible energy implications. The risk of investing in further research in the area, which could turn out to be a dead end, should be mitigated by the current results, relatively low cost of initial research and possible rewards. Finally I can't imagine a better place to carry out this research than in Scandinavia, and especially Norway which already holds a traditional role as an energy supplier to the world.

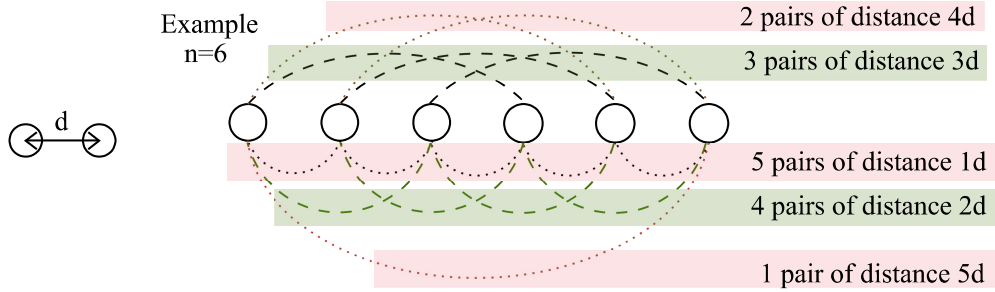
References

- [1] British Petroleum, “Statistical Review of World Energy,” Jun. 2016. [Online]. Available: <https://www.bp.com/content/dam/bp/pdf/energy-economics/statistical-review-2016/bp-statistical-review-of-world-energy-2016-full-report.pdf>
- [2] International Energy Agency, “World Energy Outlook 2016,” 2016. [Online]. Available: <http://www.worldenergyoutlook.org/publications/weo-2016/>
- [3] United Nations, “Paris Agreement,” Nov. 2016. [Online]. Available: http://unfccc.int/paris_agreement/items/9485.php
- [4] IEA Ministerial, “Ministerial Statement on Energy and Climate Change,” 2015.
- [5] NOAA National Centers for Environmental Information, “State of the Climate: Global Analysis for Annual 2016,” Tech. Rep., Jan. 2017. [Online]. Available: <http://www.ncdc.noaa.gov/sotc/global/201613> (Accessed 2017-02-28).
- [6] J. Ongena and Y. Ogawa, “Nuclear fusion: Status report and future prospects,” *Energy Policy*, vol. 96, pp. 770 – 778, 2016. [Online]. Available: <http://www.sciencedirect.com/science/article/pii/S0301421516302658>
- [7] Kikuchi *et al.*, *Fusion Physics*. Vienna: International Atomic Energy Agency, 2012.
- [8] M. Alonso and E. J. Finn, *Fundamental University Physics*, ser. Addison-Wesley series in physics. United States of America: Addison-Wesley Publishing Company, Inc, Aug. 1966.
- [9] J. W. Jewett and R. A. Serway, *Physics for Scientists and Engineers with Modern Physics*, 8th ed. California: Mary Finch, 2010.
- [10] X. Ji, “A Introduction to Nuclear Physics,” University of Maryland, 2012. [Online]. Available: <http://www.physics.umd.edu/courses/Phys741/xji/chapter7.pdf> (Accessed 2017-02-20).
- [11] M. Mansfield and C. O’sullivan, *Understanding Physics*. Chichester, England: John Wiley & Sons Ltd in assoc. Praxis Publishing Ltd, 1998.
- [12] Wikipedia, “Iron-56.” [Online]. Available: <https://en.wikipedia.org/wiki/Iron-56>
- [13] R. Chang, *General Chemistry*, 4th ed. McGraw-hill book company, 2006.
- [14] I. Cook *et al.*, “Safety and environmental impact of fusion,” *EUR (01) CCE-FU / FTC 8/5*, Apr. 2001.
- [15] F. F. Chen, *An Indispensable Truth: How Fusion Power Can Save the Planet*. Springer Science and Business Media,, 2011.
- [16] J.-S. Yoon *et al.*, “Electron-impact cross sections for deuterated hydrogen and deuterium molecules,” *Reports on Progress in Physics*, vol. 73, no. 11, pp. 116–401, 2010. [Online]. Available: <http://stacks.iop.org/0034-4885/73/i=11/a=116401>
- [17] M. Fleischmann and S. Pons, “Electrochemically induced nuclear fusion of deuterium,” *J. Electroanal. Chem.*, vol. 261, pp. 301 – 308, 1989.
- [18] S. Koonin and M. Nauenberg, “Calculated fusion rates in isotopic hydrogen molecules,” *Letters to Nature*, 1989.
- [19] S. Jones *et al.*, “Observation of cold nuclear fusion in condensed matter,” *Nature volume*, vol. 338, pp. 737 – 740, 1989.
- [20] G. Levi *et al.*, “Observation of abundant heat production from a reactor device and of isotopic changes in the fuel,” 2014. [Online]. Available: <http://amsacta.unibo.it/4084/1/LuganoReportSubmit.pdf>

- [21] L. W. Alvarez *et al.*, “Catalysis of Nuclear Reactions by mesons,” vol. 105(3), pp. 1127–1128, Feb. 1957.
- [22] K. Nagamine, *Introductory Muon Science*. Cambridge, United Kingdom: Cambridge University Press, 2003.
- [23] S. Badiei *et al.*, “High-energy coulomb explosions in ultra-dense deuterium: Time-of-flight-mass spectrometry with variable energy and flight length,” *International Journal of Mass Spectrometry*, vol. 282, pp. 70 – 76, Feb. 2009.
- [24] L. Holmlid, “Laser-induced fusion in ultra-dense deuterium d(-1): Optimizing mev particle emission by carrier material selection,” *Nuclear Instruments and Methods in Physics Research Section B: Beam Interactions with Materials and Atoms*, vol. 296, pp. 66 – 71, Feb. 2013.
- [25] L. Holmlid, “High-charge coulomb explosions of clusters in ultra-dense deuterium d(-1),” *International Journal of Mass Spectrometry*, vol. 304, pp. 51 – 56, Feb. 2011.
- [26] L. Winterberg, “Ultra-dense deuterium and cold fusion claims,” *Physics Letters A*, vol. 374, pp. 2766 – 2771, 2010.
- [27] Atomic Physics Group, University of Bergen, *Private communication*, 2018.
- [28] R. Gaillac *et al.*, “Attosecond photoemission dynamics encoded in real-valued continuum wave functions,” *Physical Review*, vol. A 93, 013410, Feb. 2016.
- [29] R. Loudon, “One-dimensional hydrogen atom,” *American Journal of Physics*, vol. 27, 649; doi: 10.1119/1.1934950, 1959.
- [30] L. Haines and D. Roberts, “One-dimensional hydrogen atom,” *American Journal of Physics*, vol. 37, 1145; doi: 10.1119/1.1975232, Nov. 1969.
- [31] H. Agueny *et al.*, “Scaling properties of field ionization of rydberg atoms in single-cycle,” *J. Phys. B: At. Mol. Opt. Phys.*, vol. 49, 245002, 2016.
- [32] L. Holmlid *et al.*, “Ultrahigh-density deuterium of rydberg matter clusters for inertial confinement fusion targets,” *Laser and Particle Beams*, vol. 27, p. 529–532, 2009.

Appendices

A Repulsion in a string



Distance between any two neighbouring particles is d . All particles are of single charge.

A pair has repulsion

$$\frac{e^2}{\text{distance}} = \frac{e^2}{d} \frac{1}{(n - \text{pairs})}$$

Where *pairs* is number of pairs at this distance. All pairs of the same distance have repulsion

$$\frac{e^2}{d} \frac{1}{(n - \text{pairs})} \text{pairs}$$

Repulsion of all pairs can be written as the sum

$$\frac{e^2}{d} \left[(n-1) + \frac{1}{2}(n-2) + \frac{1}{3}(n-3) + \dots + \frac{1}{n-1}(n-(n-1)) \right]$$

First element in bracket is for 5 pairs, second for 4, third for 3 pairs etc up to final n pair spanning the total length of the linear arrangement. The above sum can be written out as

$$\frac{e^2}{d} \left[n-1 + \frac{n}{2} - 1 + \frac{n}{3} - 1 + \dots + \frac{n}{n-1} - 1 \right]$$

which when sorted gives

$$\frac{e^2}{d} \left[n \left(1 + \frac{1}{2} + \frac{1}{3} + \dots + \frac{1}{n-1} \right) - 1 - 1 - 1 - \dots - 1 \right]$$

This can be rewritten as the sum

$$\frac{e^2}{d} \left(n \left(\sum_{k=1}^{n-1} \frac{1}{k} \right) - (n-1) \right)$$

B Matlab code

B.1 Numerical Schrödinger equation

```
% Diagonalize 1D Schroedinger equation
%-
%      [ -1/2 (d/dx)^2 + V(x) ] psi(x) = E psi(x)
%-
% in a basis of box states (sin(n*pi*x/L)
% for sufficiently large L.
% Number of x points are chosen such that functions are well defined
% Number of basis functions are determined by not observing changes when increased
format compact;
L=40; % L proportional to potential
N=400; % N defines the most rapidly oscillating wave in psi.
center=40; ctr=center; %Does not serve any purpose, but has not been removed
dx=1/250; Nx=L/(dx);

x=linspace(ctr-L/2,ctr+L/2,Nx); n=1:N; %generates resolution
xp=potential(ctr,d,Z,x); %generates potential
y=x-ctr+L/2; %shifts evaluation to start at x=0

Ham=zeros(N,N) + diag((n.*pi).^2/(2*L^2)); %Generates the hamiltonian matrix and
adds the normalized kinetic energy diagonal terms

%Potential energy terms added to hamiltonian matrix.
for j=1:N
    sinj=sin(j*pi*y/L);
    for k=j:N
        Ham(j,k)=Ham(j,k)-2.0/L*sum((sinj).*sin(k*pi*y/L).*xp)*dx;
        Ham(k,j)=Ham(j,k); %The matrix should be diagonally symmetrical.
    end;
end;
[V,D]=eig(Ham); E=diag(D); %Eigenvalues and eigenstates calculated
```

B.2 Truncation value optimization

```
%Program generates truncation values which produces "united atom" eigenvalue 1s.
Results=[];
for Z=10:1:50; %Z for loop to be replaced with single Z value if figure to be produced
Engy=zeros(1,30);
    for stp=1:1:30;
        B=50*stp; %Appropriate intervals on B for interpolation
        Schroedinger; %Solve 1s for current B to be tested
        Engy(stp)=E(1); %E(1) for proposed B
    end
B_Z=interp1(Engy,1:30,-1/2*Z^2); %Interpolates B where it produces E(1)=1/2*Z^2
B=50*B_Z; %each step in B_Z porportional to 50 increment in B.
Schroedinger; %checks the interpolated B
Results=[Results;Z 50*B_Z E(1) -1/2*Z^2] %E(1) is generated based on interpolated B.
end
save(['B_optimization','.txt'],'Results','-ascii')
%{
Figure below visually represents E(1) for different B versus 1/2*Z^2, only
works for one Z, remove "Z for loop" befor uncommenting.
figure(3);
plot(1:stp,Engy,'k-');
hold on
line([0 stp],[-1/2*Z^2 -1/2*Z^2]);
%}
```

B.3 Potential

```
function xp= potential(center,d,Z,xx)
% potential function
% with truncation B
% and distance D
% between Z center symmetrical nuclei ( Z = 1,2, .... )
% xx array is evaluation values of positions
%
load B_optimization.txt;
B=B_optimization(Z-9,2); (This is truncationvalue giving E_s1)

PNTS=center + d*(-(Z-1)/2:1:(Z-1)/2);
%PNTS is an array representing symmetrical nuclei positions.
xp=xx*0;
%xp is here generated to initially have zeros in array with number of elements equal to xx.

% Unmodified coulomb potential
for k=1:1:Z
    POTS=abs(xx-PNTS(k)).^(-1);
    xp=xp+POTS;
end

% Following variations are used for the different truncation modes:
% Truncation at Vcut (serves as minimum for all modes):
xp(xp>B)=B;

% Truncation at Vb
xp=-xp;
[peak,loc]=findpeaks(xp,xx);
top=max(peak);
bot=min(peak);
xp(xp<(bot))=bot;
xp=-xp;
xp(xp>B)=B;

% Truncation at Vmid
xp=-xp;
[peak,loc]=findpeaks(xp,xx);
top=max(peak);
bot=min(peak);
xp(xp<(bot+(bot-top)))=(bot+(bot-top));
xp=-xp;
xp(xp>B)=B;
```


B.4 Repulsion

```
%Script calculates total repulsion in string
PNTS=center+d*(-(Z-1)/2:1:(Z-1)/2);
repuls=0;
for k1=1:Z
    for k2=k1+1:Z
        repuls=repuls+1.0/(abs (PNTS(k1)-PNTS(k2)) );
    end
end;
```

B.5 Main analysis program

```
%Script to run potential.m and Schroedinger.m for range of Z and d.
```

```
tic
AllRes=[];

for Z=10:1:45;
    Stp=62;
    Energy=zeros(1,Stp);%Array to log eigen energies, one element for each step.
    Results=[];
    fprintf('\nCurrent step is evaluating for variable values:\n')
    for u=1:1:Stp
        if u<50
            d = 0.005+((u-1)*0.0015);
        elseif 50<=u & u<60
            d = 0.08+((u-50)*0.01);
        elseif 60<=u
            d = 0.18+((u-60)*0.082);
        end
        fprintf('Step %d of %d: Distance factor = %4.3f\n',u,Stp,dfactor)
        Schroedinger; %Schroedinger script solves
        for electron eigenvalues and eigenstates
        Repulsion; %Calculates sum of nuclei repulsion.
        Eneg=E<0;E=E.*Eneg; %Removes positive eigenvalues
        Energy(u) = sum(E(1:floor(Z/2)))+sum(E(1:ceil(Z/2))); %Sums eigen
        energies (2 electrons for each state)
        Binding=Energy(u)+repuls;
        Results = [Results;Z dfactor repuls Binding Energy(u) E']; %logs results for each step.

        Step_figure; %Produces and saves figure for each step. (optional)

    end
    Results( :, all(~Results,1) ) = [];
    save (['Z_',num2str(Z),'_Steps_',num2str(Stp),'.txt'],'Results','-ascii') %saves results.
```

```

%following lines produce and save PES plot of analysis.
figure(Stp+1)
plot(Results(:,2),Results(:,5),'linewidth',2,'color','r' );hold on;
plot(Results(:,2),Results(:,3),'linewidth',2,'color','b');
plot(Results(:,2),(Results(:,3)+Results(:,5)),'linewidth',2,'color','m')
line([1/(10*Stp) 1],[0 0],'linewidth',0.5,'color','k')
title(['Energies for Z=',num2str(Z),' vs. nuclei distance.']);
xlabel('Distance [a.u.]'); ylabel('Energy [a.u.]');
ylim([1.1*min(Results(:,5)) -1.4*min(Results(:,5))])
xlim([0 0.3])
legend('Binding energy', 'Repulsion', 'PES','Location', 'northeast');
set(gca,'fontsize',20);
pictname=['Z_' num2str(Z) '__Steps_' num2str(Stp) '.eps'];
pngname=['Z_' num2str(Z) '__Steps_' num2str(Stp) '.png'];
set(gcf,'paperpositionmode','auto')
comand=['print ' pictname ' -depsc'];
set(gcf,'PaperUnits', 'points');
set(gcf,'PaperPosition', [ 0 0 1000 1800]);
eval(comand);
comand=['print ' pngname ' -dpng'];
eval(comand);
set(gcf,'PaperUnits', 'points');
set(gcf,'PaperPosition', [ 0 0 1000 1800]);
[MinVal,MinIndex]=min((Results(:,3)+Results(:,5))); %locates minimum
D_at_min=[Results(MinIndex,2),MinVal]; %locates distance at minimum
save(['Minimum_D_Z_',num2str(Z),'_Steps_',num2str(Stp),'.txt'],'D_at_min','-ascii');
%saves minimum d and result energy
AllRes=[AllRes;Z Results(MinIndex,2)];
close all;
clearvars -except AllRes
end

%following produce scatter plot of all Z analysed.
figure;
scatter(AllRes(:,1),AllRes(:,2),'MarkerEdgeColor',[.09 .09 .09],...
        'MarkerFaceColor',[.28 .28 .28],...
        'LineWidth',1.5);
title('Minimum distances - cut at V_b');
xlabel('Number of nuclei')
ylabel('Nuclei distance at minimum')
ylim([0.065 0.125]);
xlim([9 30]);
set(gca,'fontsize',12);

```

```
set(gcf,'PaperUnits', 'points');
set(gcf,'PaperPosition', [ 0 0 1200 1000]);
pictname=('Minimum_Vcut.eps');
pngname=('Minimum_Vcut.png');
set(gcf,'paperpositionmode','auto')
comand=['print ' pictname ' -depsc'];
eval(comand);
set(gca,'fontsize',15);
comand=['print ' pngname ' -dpng'];
eval(comand);
save(['Min_d_database.txt'],'-ascii');
fprintf('\n Analysis complete. ');
toc
```